Winter 2-15-2023

Biogas Combustion Characteristics in a Concentric Flow Slot Burner: Effects of Co2 Concentration on Stability and Flame Structure

Maged Kiriakos
magedmicheal@aucegypt.edu

The American University in Cairo
الجامعة الأمريكية بالقاهرة

Graduate Studies

BIOGAS COMBUSTION CHARACTERISTICS IN A CONCENTRIC FLOW SLOT BURNER: EFFECTS OF CO_2 CONCENTRATION ON STABILITY AND FLAME STRUCTURE

A THESIS SUBMITTED BY

Maged Kiriakos

Advisors:-
Dr. Mohy Mansour
Dr. Amr Serag

TO THE

Master of Science in Mechanical Engineering Program

5/1/2023

In partial fulfillment of the requirements for the degree of Master of Science

Declaration of Authorship

I, Maged Micheal Kiriakos, declare that this thesis titled, "BIOGAS COMBUSTION CHARACTERISTICS IN A CONCENTRIC FLOW SLOT BURNER: EFFECTS OF CO_2 CONCENTRATION ON STABILITY AND FLAME STRUCTURE" and the work presented in it are my own. I confirm that:

- This work was done wholly or mainly while in candidature for a research degree at this University.
- Where any part of this thesis has previously been submitted for a degree or any other qualification at this University or any other institution, this has been clearly stated.
- Where I have consulted the published work of others, this is always clearly attributed.
- Where I have quoted from the work of others, the source is always given. Except for such quotations, this thesis is entirely my own work.
- I have acknowledged all main sources of help.
- Where the thesis is based on work done by myself jointly with others, I have made clear exactly what was done by others and what I have contributed myself.

Signed: 

Date: 5/1/2023

Abstract

Biogas combustion is affected by the concentration of carbon dioxide. The successful applications of Biogas as a sustainable renewable alternative fuel produced from waste depend on its combustion stability, heat release, and pollution level. The aim of the current study is to apply new combustion technology and study the stability and combustion characteristics of natural gas with different percentages of carbon dioxide from 0 to 40% simulating biogas fuel. The stability characteristics and the temperature profiles of turbulent planar flames at different levels mixture inhomogeneity are investigated and presented in this work. The flames are created in a newly developed concentric flow slot burner, CFSB, for different mixtures of 0, 10, 20, 30, and 40% of CO_2 in natural gas. The stability characteristics, and the flame temperature measurements were carried out for different levels of mixture inhomogeneity and for the natural gas- CO_2 mixtures. The main parameters of the current investigations are the mixture equivalence ratio, the Reynolds number, the level of mixture inhomogeneity, the air-to-fuel velocity ratio, and the air-to-fuel momentum ratio.

The flames show highest stability at a partial premixing ratio equal to 5 for mixture inhomogeneity between fully premixed and non-premixed cases. At this level, the highest stability may be attributed to the generation of higher level of radicals from the rich pockets of the mixture. Lower stability was recorded at higher levels of CO_2 concentration in the fuel, as expected due to the lower level of the fuel heating value and the temperature diluting effect of CO_2. On the other hand, the stability is decreasing almost linearly by increasing the momentum ratio for all cases of CO_2 concentration and all cases of mixture inhomogeneities. The temperature profiles show a reduction of the temperature level by increasing the CO_2 concentration, as expected.

The current work shows the advantage of using turbulent planar flames with an inhomogeneous mixture to stabilize biogas for practical combustion systems. So, biogas can successfully replace fossil fuels for a sustainable energy supply.

Acknowledgements

"The God of heaven will prosper us. Therefore we, his servants, will arise and build" Nehemiah 2:20.

No words can be sufficient to express my gratitude and indebtedness to my family who have been encouraging me throughout my whole life and behind every success I have done.

To Prof. Mohy Mansour, I would like to express my sincerest appreciation and gratitude for providing your valuable advice during the whole research period. Your advice & high-standard instructions have encouraged me to reach my extreme potential during all preparation stages of this thesis. Moreover, I am most grateful for your help, understanding and support. Your supervision will always be appreciated.

To Prof. Amr Serag and Prof. Hanadi, I am greatly honored to express my thanks for your help and my deepest appreciation for giving me important advice. I am grateful for your advice with kind guidance throughout the whole work until this work came to existence.

I want to thank the American university for funding this important research which came out with very useful and efficient solutions for biogas combustion. Finally, I would like to dedicate this work to all Staff Members and My Colleagues in Faculty of Engineering – American University in Cairo and Cairo University, for their valuable suggestions and fruitful cooperation.

Contents

List of Figures

List of Tables

List of Abbreviations

LD	*Premixing Ratio Length/Diameter of a hollow chamber*
CFSB	*Concentric Flow Slot Burner*
BSEC	*Brake Specific Energy Consumption*
C	*Celsius*
MN	*Methane Number*
LHV	*Lower Heating Value*
ST	*Spark Timing*
CAD	*Crank Angle in Degrees*
A/F	*Air to Fuel Ratio*
rpm	*Revolution per Minute*
ID	*Ignition Delay*
atm	*Atmospheric Pressure*
NG	*Natural Gas*
BG	*Biogas*
Vr	*Velocity Ratio*
RMS	*Root Mean Square*
Re	*Reynolds Number*
Q	*Load (W)*
Z	*Axial distance above burner's nozzle*
I	*Momentum Ratio*
slm	*Standard Liter per Minute*

List of Symbols

CO_2	*Carbon Dioxide*
$O2$	*Oxygen*
Φ	*Equivalence Ratio*
$\boldsymbol{\Theta}$	*Nozzle Cone Angle*
U_j	*Jet Velocity*
Re_j	*Jet Reynolds number*
X_{CO2}	*Carbon Dioxide Mole Fraction*
X_{CH4}	*Methane Mole Fraction*
X_{Air}	*Air Mole Fraction*
Y_{air}	*Air Mass Fraction*
T	*Temperature*
P_{atm}	*Atmospheric Pressure*
M_{air}	*Air Molecular Mass*
M_{CH4}	*Methane Molecular Mass*
M_{CO2}	*Carbon Dioxide Molecular Mass*
ρ_{air}	*Air Density*
ρ_{CH4}	*Methane Density*
ρ_{CO2}	*Carbon Dioxide Density*
ρ_{fuel}	*Fuel Density*
Q_{air}	*Air Volume Flow Rate*
Q_{CH4}	*Methane Volume Flow Rate*
Q_{CO2}	*Carbon Dioxide Volume Flow Rate*
m°_{Air}	*Air Mass Flow Rate*
m°_{CH4}	*Methane Mass Flow Rate*
m°_{CO2}	*Carbon Dioxide Mass Flow Rate*
m°_{mix}	*Whole Mixture Mass Flow Rate*
$A/F_{St.}$	*Stoichiometric Air to Fuel Ratio*
A/F_{Actual}	*Actual Air to Fuel Ratio*
L	*Burner Exit Slot Length*
W	*Burner Exit Slot Width*
W_{air}	*Air Slot Width*
W_{fuel}	*Fuel Slot Width*
D_h	*Hydraulic Diameter*
U_{mix}	*Velocity of the Whole Mixture*
μ_{mix}	*Viscosity of the Whole Mixture*
V_r	*Air to Fuel Velocity Ratio*
I	*Air to Fuel Momentum Ratio*

Chapter 1

Introduction

1.1 Biogas History and Production:

Transportation and power plant sectors are mostly responsible for the highest CO_2 emissions across the globe, as they depend on burning large amounts of fossil fuels. Such amounts of CO_2 emissions from combustion remain in the atmosphere which later absorbs heat coming from sun, thus caging the earth with a hot layer causing global warming. Reliance on renewable sustainable sources of fuel is needed. The aim of this report is to investigate the compatibility of biogas in combustion process, as it is considered as renewable fuel alternative that originates from the secretion of living animals, plants, and even humans [15]. Less carbon atoms availability in biogas ensures the low emissions of CO_2 after being used as an energy input, which in turn will reduce the global warming effect. Not only does biogas act as a sustainable environmentally friendly energy source, but also helps in many various ways of wastes disposal. For instance, in the US, the amount of manure produced every year exceeds one billion tons and it is mostly thrown in lakes and outdoor storage. Consequently, greenhouse gases are released in air like methane and nitrous oxides which highly contribute to warming the earth up [24]. Simsek et al. [25] used a spark ignition engine supplied by biogas to compare the proportions of the constituents of exhaust emissions with the constituents of the exhaust coming from normal combustion of gasoline. The emissions were found to decrease by 48.96%, 56.42%, and 63% for nitrogen oxide (NOx), carbon monoxide, and hydrocarbon respectively. Despite the fact that biogas increases the combustion period and causes

ignition delay due to the presence of CO_2, the amount of NOx emissions on the other hand was greatly reduced [26].

Biogas in general contains 50-80% methane and 20-40% CO_2 depending on the feedstock used in the digesters. So, starting from 1970, attempts of relying on biogas became large due to the inflation of oil prices during that time which in turn encouraged researchers to find other fuel alternatives like biogas. Biogas gained interest across the world due to the low construction costs needed. Besides, digesters can be quickly and easily built even by unskilled local labor [14]. In the first half of 1980s, an increase in biogas usage was found in Asia, Africa, and Latin America. The government in China encouraged the spread of biogas use in rural areas and helped in installing more than seven million digesters. During the turn of this century, a fast increase in number of digesters registered was noticed as shown in figure 1, and by 2007 the number of digesters was found to be 26.5 million [1].

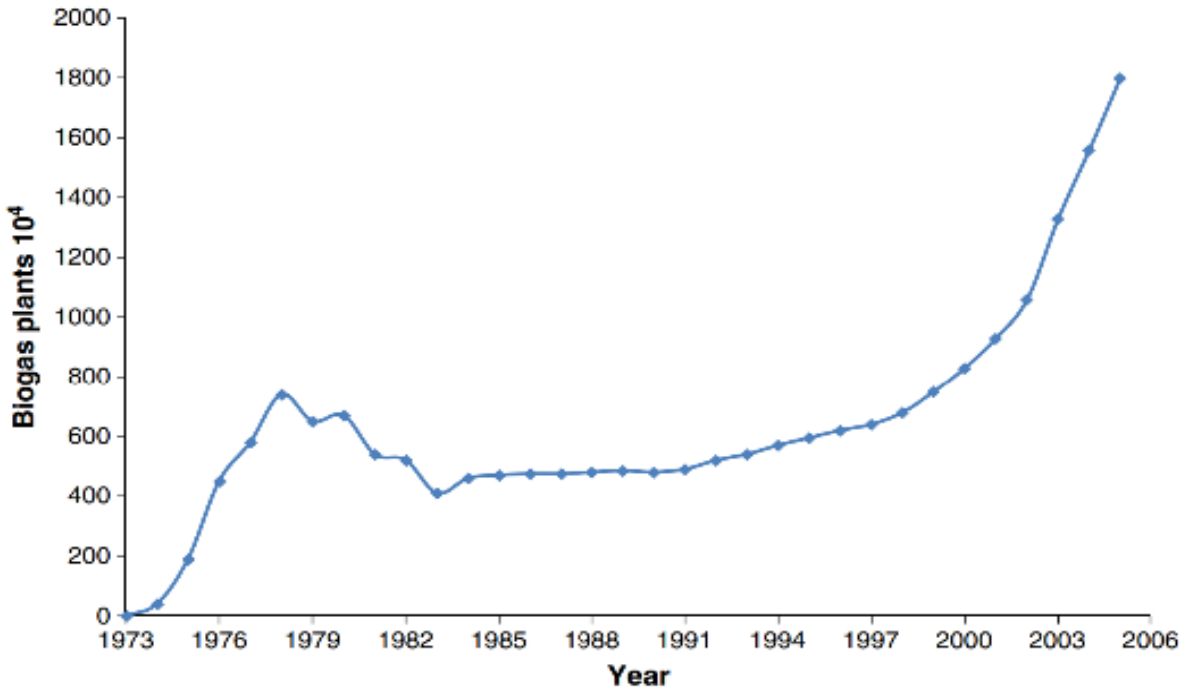

Figure 1: Number of biogas plants in China across years [1]

Over the last 10 years, the number of biogas plants has increased resulting in more biogas production. The number of digesters increased to 6227 by 2009 in Europe. It then doubled to 13,812 by 2012. A 30% increase in the number of digesters was recorded after another five years reaching a total number of 17,783 plants, as shown below in figure 2 which illustrates the distribution of digesters among the top 15 countries in Europe [1]. The bar chart in figure 3 shows the production of Biogas in mega tons of oil equivalent for every continent each year starting from 2012. As shown in figure 3, the biogas production over the world increases almost linearly over the years and that Europe counties became the top producer of biogas followed by Asia as it almost produces half the amount.

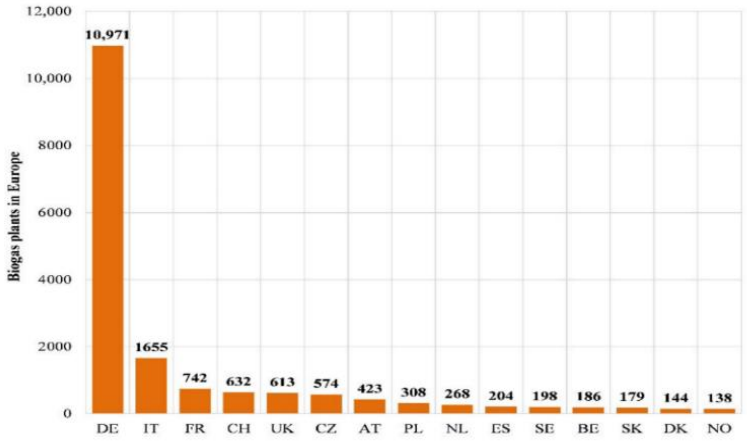

Figure 2: Number of biogas plants in Europe countries [1]

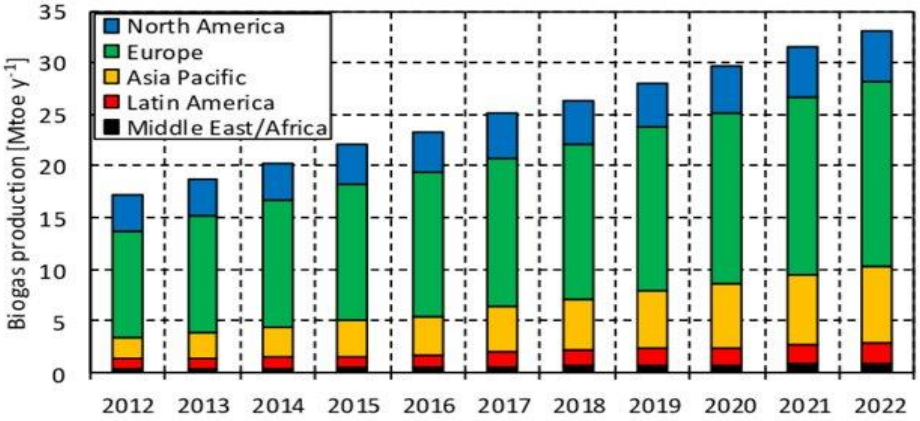

Figure 3: Biogas Production in Mega Tons of oil equivalent per year from 2012 up to 2022 [19]

Biogas is produced through some steps inside the digester. Firstly, complex carbohydrates, proteins, and lipids are degraded by the extracellular enzymes in a process called hydrolysis. The products from the hydrolysis process are converted to hydrogen, acetic acid, and CO_2 in a process called acidogenesis. Next is the final step where anaerobic bacteria interfere with the acidogenesis byproducts to control the production of methane gas. Some digesters operate in mesophilic condition where the temperature range is 20-40C or thermophilic condition where the temperature is above 40C depending on the type of feedstock. Methane is produced along with CO_2 and sludge which can be used as a fertilizer later [1].

1.2 Limitations of Biogas

Aside from methane and CO_2, biogas may contain traces of impurities like hydrogen, hydrogen sulfide, ammonia, oxygen, carbon monoxide and nitrogen. Before using biogas, harmful and toxic impurities must be removed by chemical or physical means like desulphurization or membrane segregation respectively.

The CO_2 in biogas constituents decreases the calorific value or the lower heating value of the biogas fuel. This happens because CO_2 as an inhibitor impedes the combustion process as it acts as a diluting agent to the fuel. CO_2 hinders the reaction since it is not flammable as methane and at the same time it absorbs the reaction heat which in turn decreases the rate of reaction [1]. So, the flammability limits in biogas are different than pure methane because of the difference in equivalence ratio. Flammability limits indicates between what limits the proportion of combustible gases is flammable [13]. Gas mixtures may contain inert, oxidizing, and combustible gases which are flammable under certain conditions

based on mixture fractions of each component [12].

CO_2 in biogas decreases the LHV, which leads to a decrease in the amount of heat produced from the complete biogas combustion. On the other side, biogas increases the Methane Number (MN) because of its constituents which enhances knocking resistance. For instance, hydrogen has MN of 0 while methane has MN of 100, which means if we mix 60% methane with 40% hydrogen then the MN at the end will be equivalent to 60. Having lower MN means less CO_2 emissions, higher flame speed thus higher rate of heat release, but on the other side it will lead to lower compression ratio in engines and less knocking resistance. However, if 60% methane was mixed with 40% CO_2 then the equivalent MN will be 140, resulting in higher knocking resistance and higher compression ratios up to 17.6:1 can be achieved in some engines.

The main drawback of biogas is that CO_2 as one of its proportions increases the self-ignition temperature which causes more delay than normal [16]. Having lower CO_2 proportion in the input fuel leads to increase in peak pressure in cylinder and LHV which helps in reducing brake specific fuel consumption. It is very important to have consistency in biogas mixture proportions for the engine to adapt on [16]. Because if this was not the case, fuel consumption and emissions will increase due to the mixture variations in each cycle [2].

The next part of the report will study several research works done in the field of biogas and how it is related to the current work. Then, the experimental technique and apparatus implemented will be discussed to understand how the measurements are extracted. In the discussion section, measurements obtained are

processed by some equations and plotted to reach solid conclusions about the conditions at which biogas flames are highly stable.

Chapter 2

Background and Literature Review

Biogas combustion characteristics are very important to study, so as to reach a solid conclusion about the conditions under which optimal parameters will the biogas flame be stable. Researchers around the world studied the use of biogas as fuel by different techniques of combustion like feeding it to engines, or to burners with various geometries.

2.1 Biogas in Combustion Engines

Donatas et al. [2] investigated the effect of using bigas as a fuel on spark ignition engine. Different concentrations of CO_2 were used to see how the engine's efficiency would be affected. Donatas applied two cases of spark timing (ST), as he tried to compare between using a constant spark time occurring at 26 crank angle degrees (CAD) and a spark timing which is optimal for every biogas mixture. This 26 CAD was used as it is the optimal ST for a normal fuel not including CO_2. The experiment was conducted on all biogas mixtures with fixed engine speed of 2000 rpm, 15% opened throttle valve, and stoichiometric A/F ratio. Table 1 shows all the biogas mixtures with different CO_2 concentrations, and the corresponding parameters used for each mixture, like the LHV, stoichiometric A/F ratio, and optimal crank angle for each biogas mixture [2].

Table 1: Biogas mixtures and their corresponding MN and ST [2]

Marking	CO_2, vol%	CH_4, vol%	*LHV*, MJ/kg	Methane Number	Stoichiometric A/F Ratio	ST, CAD BTDC [1]	
						Constant	Optimal
BG0	0	100	50.0	100	17.2	26	26
BG20	20	80	29.7	118	10.2	26	30
BG40	40	60	17.7	140	6.1	26	35
BG50	50	50	13.4	151	4.6	26	40

[1] CAD BTDC—crank angle degrees (CAD) before top dead center (BTDC).

Temperature and pressure were reported in all cases to see how they vary when ST and biogas concentrations are changed. As shown in figure 4, the maximum pressure rise was obtained when biogas of 20% CO_2 and optimal ST are applied. This rise corresponds to 2.7% of the maximum pressure achieved by a fuel with 0% CO_2. Increasing the CO_2 concentration further and using optimal ST, resulted in declining the pressure rise by 16.5% and 24.5% when using biogas with 40% CO_2 and 50% CO_2 respectively. Such results are much better in comparison with using a constant ST at constant crank angle of 26, as in such case the optimum pressure was decreased by 18.9%, 56.6%, and 72.9% when using biogas with CO_2 concentrations of 20%, 40%, and 40% respectively. The low combustion speed and the longer time need for flame formation are the main reasons behind such excessive pressure drop [2].

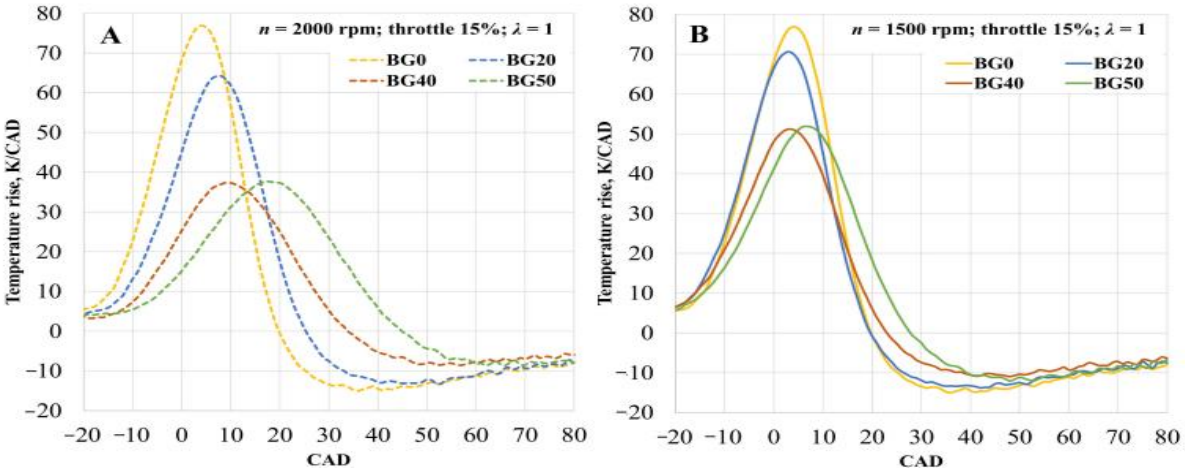

Figure 4: A & B graphs show Curves of temperature against CAD at constant ST and optimal ST respectively [2]

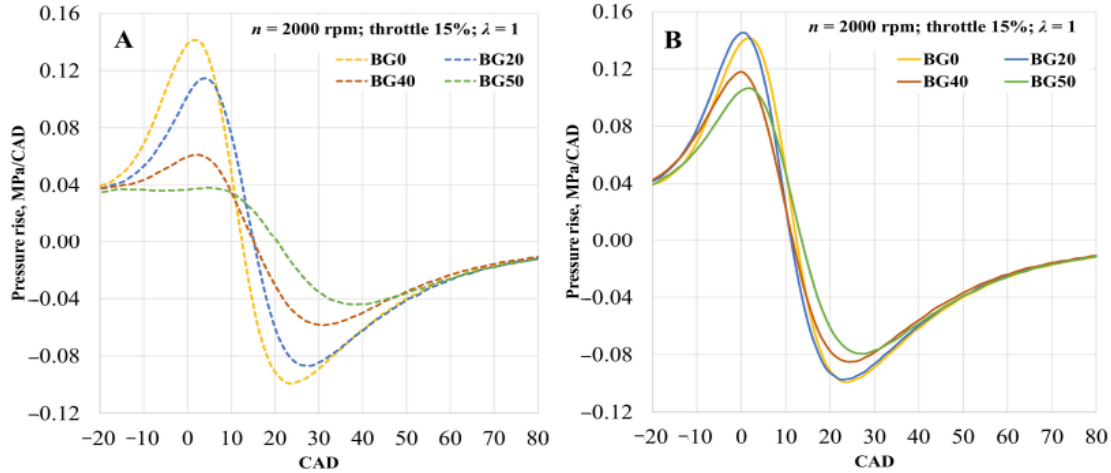

Figure 5: A & B graphs show Curves of Pressure against CAD at constant ST and optimal ST respectively [2]

Three important conclusions were reached. Firstly, the brake specific energy consumption (BSEC) increases at 26 constant crank angles because the LHV is further decreased by 64.8% and 73.6% when using CO_2 concentrations of 40% and 50% respectively. After using optimal ST, the BSEC was further enhanced by 6.39% and 16.6% for the same mixtures respectively in comparison with constant ST. Secondly, an increase of exhaust losses by 1.6%, 3.7%, and 8.7 % was noticed when using constant crank angle of 26 under 20%, 40%, 50% CO_2 biogas fuel concentrations respectively. This happened because increasing CO_2 concentrations result in longer combustion period. Finally, after assessing the amount of CO_2 formed from methane combustion under optimal ST, it was noticed that CO_2 emissions were increased by 3.1%, 11.8%, and 13.8% when using biogas with 20%, 40%, and 50% CO_2 concentrations respectively. This finding was because of the LHV of biogas fuel which is needed in greater amounts than normal to have the same power output achieved by pure methane [2].

Performance of a compression ignition engine fueled by biogas was investigated under the effect of changing oxygen concentration by Karen et al. [9]. A

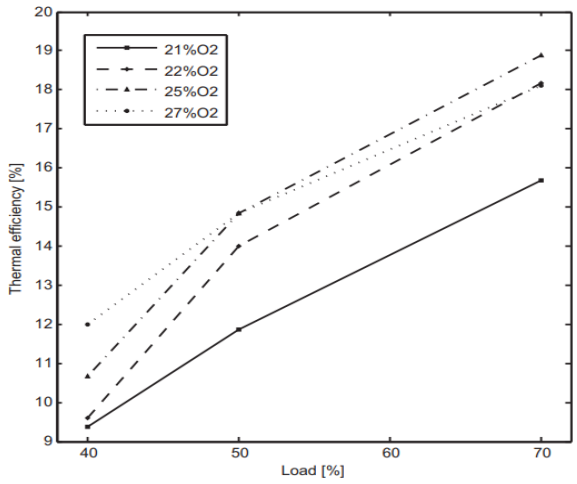

Figure 7: Graphs of thermal efficiency versus load at different O2 levels [9]

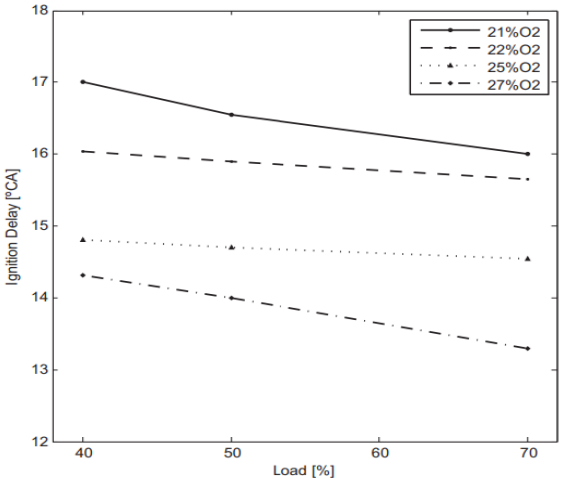

Figure 6: Graphs of ignition delay versus load at different O2 levels [9]

fixed mixture of biogas with 40% CO_2 and 60% methane concentrations was used, and the engine load was evaluated at oxygen concentrations ranging from 21% to 27%. Values of thermal efficiency, ignition delay, and methane emissions were measured and compared to normal oxygen concentration of 21% present in the atmospheric air [9].

As shown in figure 7, the ignition delay duration was decreased when the oxygen enrichment level was increased at all engine loads of 40%,50%, and 70% out of the possible full load. Such acceleration in pre ignition in diesel engine happened because of more oxygen availability during the combustion process. As seen from the ignition delay graph, that even 1% increase of oxygen level beyond the oxygen level present in atmospheric air resulted in lower ignition delay, thus achieving higher engine thermal efficiency. Also, the thermal efficiency was improved by increasing the oxygen level in the fuel as seen in figure 6. This happened due to the overall increase in mixture temperature which resulted from higher speeds of flame propagation [9].

The pressure was also increased for all engine loads when the oxygen level was increased in the intake as shown in figure 8. Maximum pressure recorded at 25% and

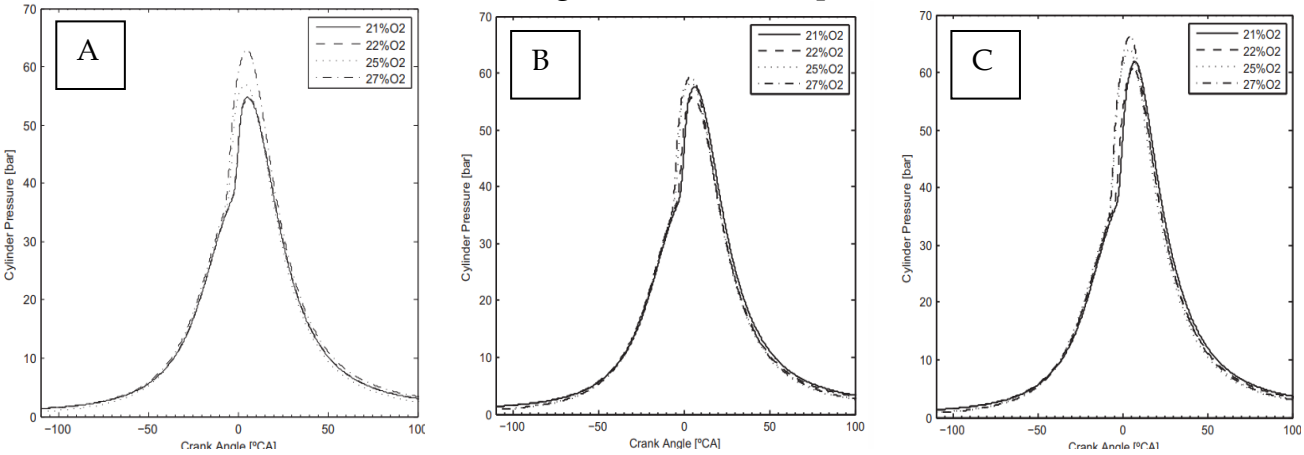

Figure 8: Graphs A, B, C show cylinder pressure against CAD at different engine loads of 40%, 50%, and 70% respectively [9]

27% oxygen levels was more than the oxygen level in atmospheric air. The higher fuel reactivity and the shorter ignition delay led to such an increase in pressure. But the difference in maximum pressure was not noticed between 22% and 21% oxygen levels although the ignition delay was reduced [9].

The main conclusion drawn from this research is that increasing oxygen level during combustion of biogas enhances the stability of reaction process. Besides, having more oxygen helped in attenuating the low flame speeds and temperatures which are the main drawbacks behind using biogas. Not only the ignition delay and thermal efficiency were improved, but also the methane emissions decreased [9].

The effect of different CO_2 concentrations on flame geometry was investigated by Fandi et al. [8]. CO_2 concentrations of 0%, 10%, 20%, 30%, 40%, and 50% were used to have different biogas mixtures. Mixing CO_2 and methane was achieved first before feeding the burner with the biogas fuel mixtures. Oxygen from one source is mixed with biogas mixture from the other source inside a burner with a nozzle exit of 5 mm in diameter. A tripod with a high-speed camera mounted on was set to capture

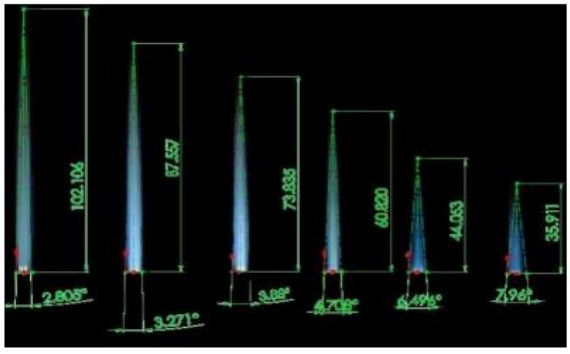

Figure 9: Heights and angles of flames at different CO_2 compositions (0%-50%) [8]

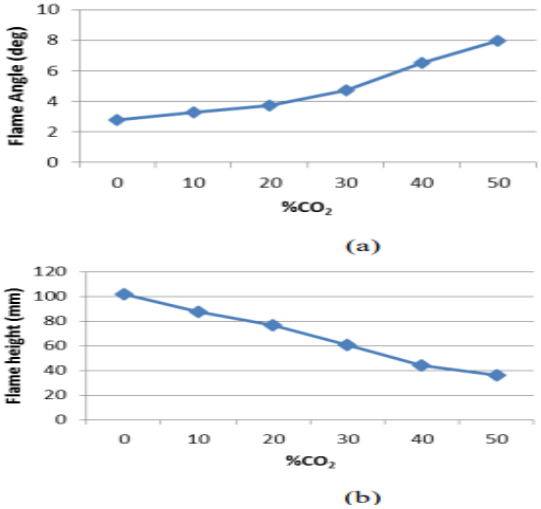

Figure 10: Trend curves showing variations of flame angle and height at different CO_2 compositions in figures (a) & (b) respectively [8]

images. The mixture was ignited once the stoichiometric A/F ratio for all the CO_2 concentrations was adjusted. Two main parameters were measured as shown in figure 9, which are the flame height from flame base to flame tip, and second the flame tip angle magnitude [8]. Results as shown in figure 10, show that increasing CO_2 concentrations lead to a linear decrease in flame height and a linear increase in flame tip angle. The difference in flame tip angles and flame heights can be observed in figure 9 [8].

The speed of flame propagation in a spark ignition premix flame powered by biogas was evaluated by Anggono et al. [10]. Different biogas mixtures with different CO_2 concentrations were employed to investigate how it affects the flame velocity. Flame characteristics were recorded by high-speed camera and a glass tube which surrounds the flame (60 mm inner diameter by 300 mm heigh dimensions). Table 2 shows the five different CO_2 concentrations used along with the corresponding recorded flame height and time duration. The flame speed was calculated by dividing the flame height by the traveling time. At stoichiometric A/F ratio, atmospheric pressure, and room temperature the results show that flame speed decreases when the CO_2 concentration is increased. In figure 11, it is clear that the flame traveling distance decreases when CO_2 concentration is increased. This happened because of the low combustion temperature reached coming from the fact that CO_2 absorbs and dilutes the combustion heat [10].

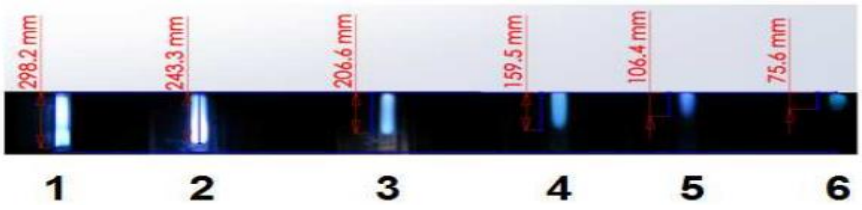

Figure 11: Measuring heights of different flame compositions [10]

Table 2: Distance and time were recorded at different flame compositions [10]

Picture No.	CO_2 (%)	Time (ms)	Distance (mm)	Flame Propagation Speed (m/s)
1	0	4.17	298.2	71.5
2	10	4.17	243.4	58.4
3	20	4.17	214.4	49.5
4	30	4.17	182.2	38.3
5	40	4.17	106.5	25.5
6	50	4.17	75.6	18.1

The effect of inhibitors present in biogas mixture and pressure on laminar burning velocity and flammability limits was studied also by Anggono et al. [11]. Spark ignited premix combustion was employed and the flames were continuously recorded by a high-speed camera to calculate the expansion rate of the flame. A fan-stirred vessel for combustion was used to create high pressure. All flames were operated at room temperature but at different equivalence ratios starting from low to high flammability limits. Four sets of flames were conducted to see the effect of both reduced pressure and inhibitors in biogas on flame laminar velocities. The four sets are flames at reduced pressure without inhibitors, reduced pressure with inhibitors, atmospheric pressure without inhibitors, and lastly atmospheric pressure with inhibitors with all sets ranging from low to high flammability limits. The reduced pressure used was 0.5 atm. A 380 mm vessel diameter as shown in figure 12 was used and fuel with different mixtures along with dry air were injected at the required pressures. As the combustion starts, the pressure transducer inside the vessel was able to record pressure at different time instants and create a graph of pressure versus time afterwards. The camera was also able to capture the flame expansion at very short time intervals of milli seconds to accurately calculate the rate of increase of the radius. Figure 13 represents flame snap shots for inhibitor less flame at different equivalence ratios, where all flames are recorded at the same reduced pressure [11].

At the normal situation, when inhibitor is absent and atmospheric pressure is applied, the range of equivalence ratios for flame operation was 0.6 to1.3. Below 0.6 any flame will be extinguished due to the low quantity of methane, which is not enough to ignite the mixture [13], while above 1.3 the methane amount is too much to be burnt at the same time. If the same conditions are applied but with the presence of the inhibitor, the equivalence ratio will be narrower ranging from 0.6 to 1.2 instead. This happened because inhibitors present like CO_2 is used to absorb more heat which

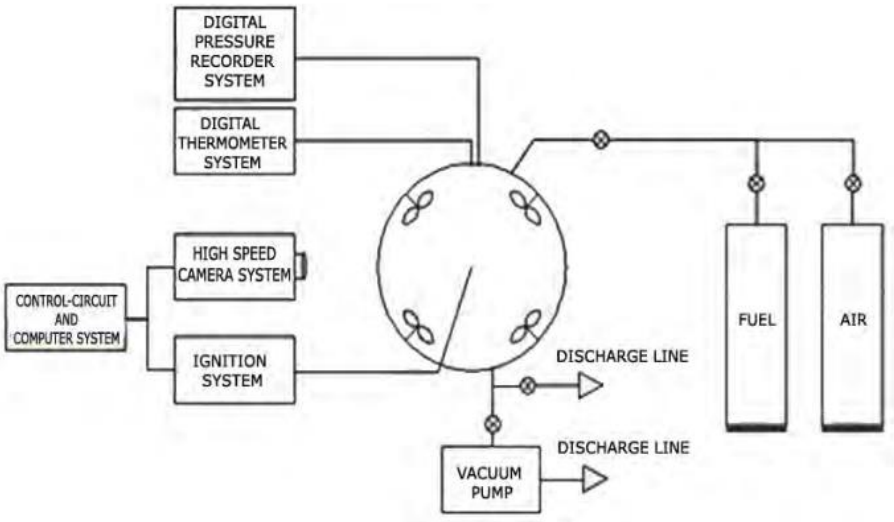

Figure 13: Schematic diagram showing the vessel connected to air and fuel supplies [11]

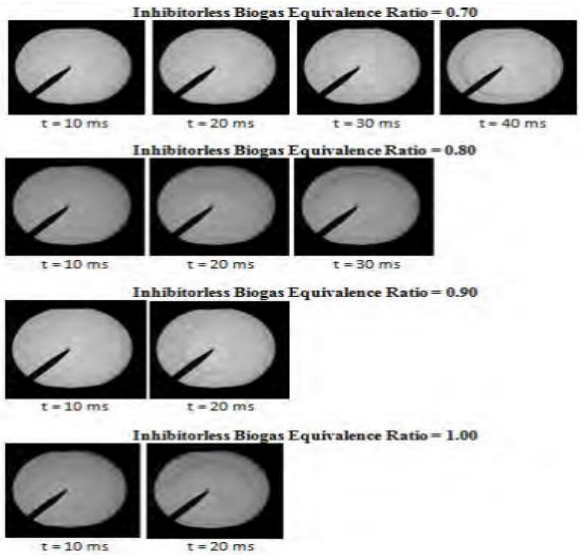

Figure 12: Snap shots of flame at progressive time instants made at different equivalence ratios [11]

is needed at high equivalence ratios to ignite more methane present in the mixture. Figure 14 shows that using fuel with and without inhibitors affects the laminar burning velocity. The presence of CO_2 as an inhibitor decreased the laminar velocity level at both levels of pressure. However, the laminar burning velocity was further enhanced by applying reduced pressure of 0.5 atm instead of 1 atm. This is due to the fact that lower pressure shortens the time for diffusion and increases thermal diffusivity, thus improving the laminar burning speeds [11].

2.2 Biogas Flames in Burners

There are three flame types that can be produced by burners which are non-premixed, partially premixed, and premixed flames of air with Natural Gas (NG). It was proven experimentally at some degree of partially premixing between air and NG that highest flame stability was recorded [17]. In Partially premixed flames, three types of reaction zones can be found creating three flame types at the same time which are lean premixed, rich premixed, and diffusion flames. This structure is called "Triple Flames" and it affects the stability of partially premixed flames propagation. Elbaz et al. [17] investigated the effect of changing the premixing ratio (LD) over the flame

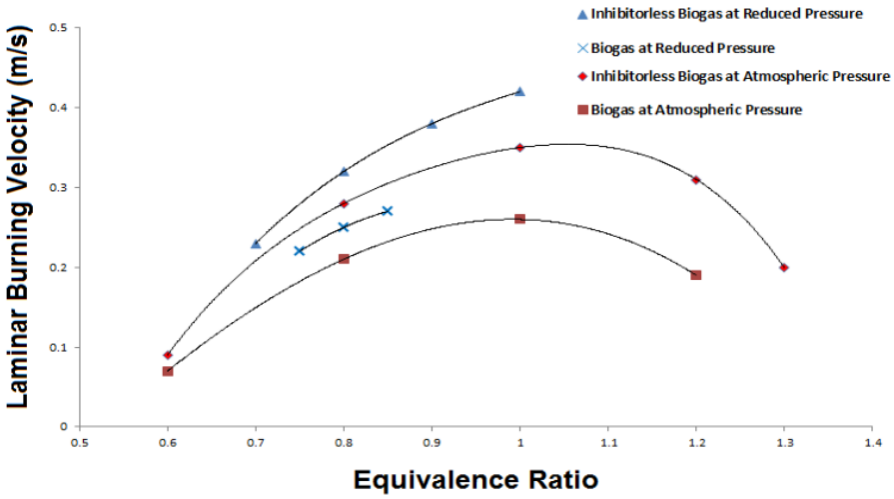

Figure 14: Plot of laminar burning velocity against equivalence ratio at different conditions of pressure and fuel mixtures [11]

structure using concentric flow nozzle burner. The burner consists of inner and outer tubes where the air exits from the inner tube and the NG exits from the outer tube [17]. To achieve some degree of partial premixing the exit of the outer tube was placed above the exit of inner tube by some length called LD. It was investigated that the highest degrees of stability could be reached at LD = 5 [3].

After the promising results were obtained, came the idea of increasing the concentric burner diameter. It was found that increasing the diameter has increased the flame stability more and more. So, Mansour et al. [18] developed a burner with a rectangular slot exit instead to achieve a nozzle with an infinite diameter. This burner was a modified version of Wolfhard-Parker slot burner to eliminate the effect of burner diameter. Two-dimensional flame sheets can be obtained from such rectangular slot burner, which can help more in studying the mixture homogeneity of partially premixed flames. Such burner consists of 2 outer thinner rectangular slots responsible for fuel supply while the inner thicker slot responsible for air supply and all slots are having equal length of 60 mm. To achieve partial premixing, hollow chambers of different heights can be mounted at a time to have different premixing ratios (LD).

Two rectangular burner slots were designed to have different exit areas. The first design was to have two NG exits of 1 mm thickness and one air exit of 6 mm thickness, so it was called 1-6-1 burner as the air exit is sandwiched in between the fuel exits. The second design was to have NG and air exits of 2 mm and 4 mm respectively, so this burner was called 2-4-2. These designs were made to change the air to fuel velocity ratio, which is controlled by the different area exits in both burners

under maintaining the same equivalence ratio. This research proved at the end that both parameters air to fuel velocity ratio (Vr) and premixing ratio (LD) were the main dominant parameters affecting the mixing process and thus the flame stability. Enhanced mixing with less variations in mixture fraction can be achieved by increasing the Vr. Also, increasing Vr by changing the slot burner maintaining the same equivalence ratio showed that LD effect was minor. Adding to this, using propane instead of methane as an input fuel resulted in attaining higher velocity ratios thus enhancing the homogeneity of the mixture.

To study more the mixture fraction at the base of the stabilization region, Mansour [4] tested three partially premixed flames at different Reynolds number and equivalence ratio to see how the level of mixture fraction differs from flame to another. The conclusion reached was that there exists a unique level of mixture fraction at the stabilization point which is found in all three flames. Which means that the flame propagation controls the stability of lifted partially premixed flame propagation. This stabilization point is achieved by the triple flame structure which was detected in all the three flames [4].

Table 3 shows three types of flames having different parameters in terms of equivalence ratio, jet Reynolds number, mixture fraction, and power output. OH radical was used to calculate the mean velocity and rms of velocity fluctuations at the burner tip. In table 4, the values of rms and mean velocity at the tip of the burner are very close to each other. Such Results prove that the flow field structure doesn't differ from flame to another at the stabilization point [5].

Table 3: Record of flame properties at different flame mixtures [5]

The main parameters of the investigated flames

Flame	U_j (m/s)	ϕ_j	Mixture fraction f_j	Re_j	Range of lift-off height (H/d)	Q^0 (kW)
PF1	4.74	4.52	0.208	2445.97	6–6.75	2.39
PF2	7.45	5.69	0.249	3633.62	6.5–8.75	4.39
PF3	11.03	7.37	0.3	5036.22	10–12.5	7.57

Table 4: RMS of velocity recorded for each flame [5]

The mean and rms of the velocity at the flame base, V_{tp}, in all flames

Flame	Mean (m/s)	Rms of V'_{tp} (m/s)	Rms/mean
PF1	1.537	0.930	0.605
PF2	1.609	0.961	0.600
PF3	1.608	0.975	0.607

Various techniques were implemented in different burner designs just for the sake of increasing stability in partially premixed flames. High flame stability means having combustion that is more intense, thus attaining high burner capacity. One of these techniques is to mount a cone at the burner exit and watch the flame behavior as the cone angle changes. Cone angles of 10, 15, 20, 25, and 30 were used by Mansour [5] to see the relation between jet velocity and equivalence ratio at each cone angle. All the flames were given the same chance of partial premixing that was attained by using LD5. The results show that at smaller cone angles, the temperature of the cone wall is increased because the flame tends to touch the cone. Having higher cone temperature gives the flame more stability at the burner exit. Figure 15 shows three photographed flames at cone angles of 20, 25, and 30 (PP20I, PP25I, PP30I) from left to right. The parameters used for producing these flames are recorded in table 5, which includes the jet velocity, jet equivalence ratio and heating rate for each flame. The flame images show that at smaller cone angle the flame touches the wall. In figure 16a, it is obvious that higher stability is reached at the least cone angles as high jet velocities can be achieved at lowest equivalence ratios. Also, in figure 16b the relation between jet velocities and the cone angles was found to be following a parabolic equation [5].

To study the effect of cone angles at constant equivalence ratios and jet velocity, another set of partially premixed flames were used (PP30I, PP25II, PP20II). As shown in table 5, the flames were studied at jet equivalence ratio of 7.54 and jet velocity of

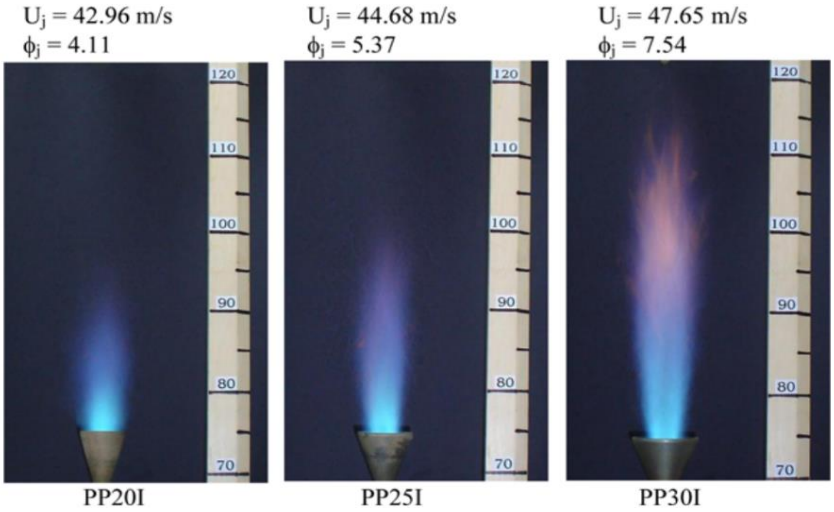

Figure 15: Flames at different cone angles and jet velocities [5]

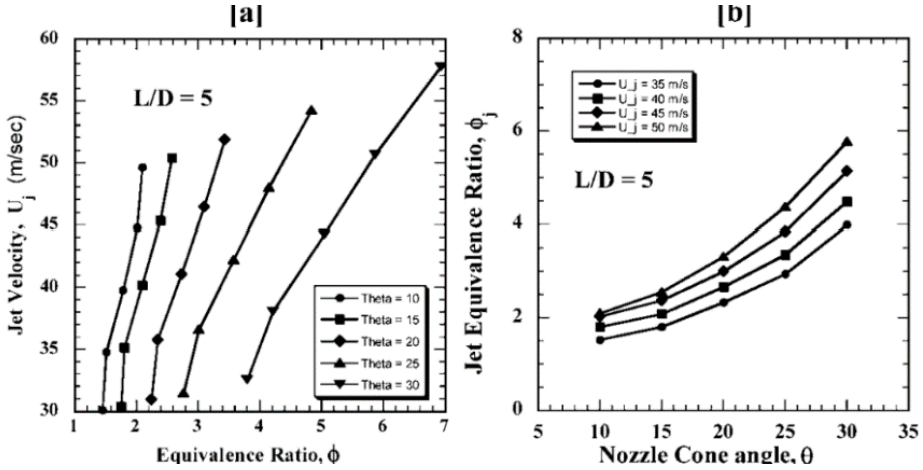

Figure 16: a) Trends of jet velocity against equivalence ratios at fixed cone angles. b) Curves of jet velocity against increasing cone angles at fixed levels of jet velocity [5]

Table 5: Last three flames tested at fixed values of jet velocity and equivalence ratio but different cone angles [5]

Flame	U_j m/s	ϕ_j	θ	RD	Q°kW
PP20I	42.96	4.11	20	0.50	28.8
PP25I	44.68	5.37	25	0.50	37.7
PP30I	47.65	7.54	30	0.50	53.1
PP25II	47.65	7.54	25	1.12	53.1
PP20II	47.65	7.54	20	1.77	53.1

47.65 m/s. Radial and axial graphs along the nozzle exit versus temperature, carbon monoxide, and oxygen were created as shown in figure 17. The graphs show that carbon monoxide concentration and temperature increase by increasing the cone angle, while oxygen concentration decreases. These results validate the flame shape obtained in figure 15, as more air is entrained when cone angle is increased thus stretching axially and squeezing the stabilization core [3].

Another technique to enhance the stability of partially premixed flames is to create an air co-flow surrounding the burner exit as suggested by Elbaz et al. [6]. Air co-flow velocities of 5 m/s, 10 m/s, and 15 m/s were used and compared to a normal case without air co-flow. Lower and upper limits of flame blowout were recorded at specific values of jet Reynolds number for each premixing ratio LD. As shown in

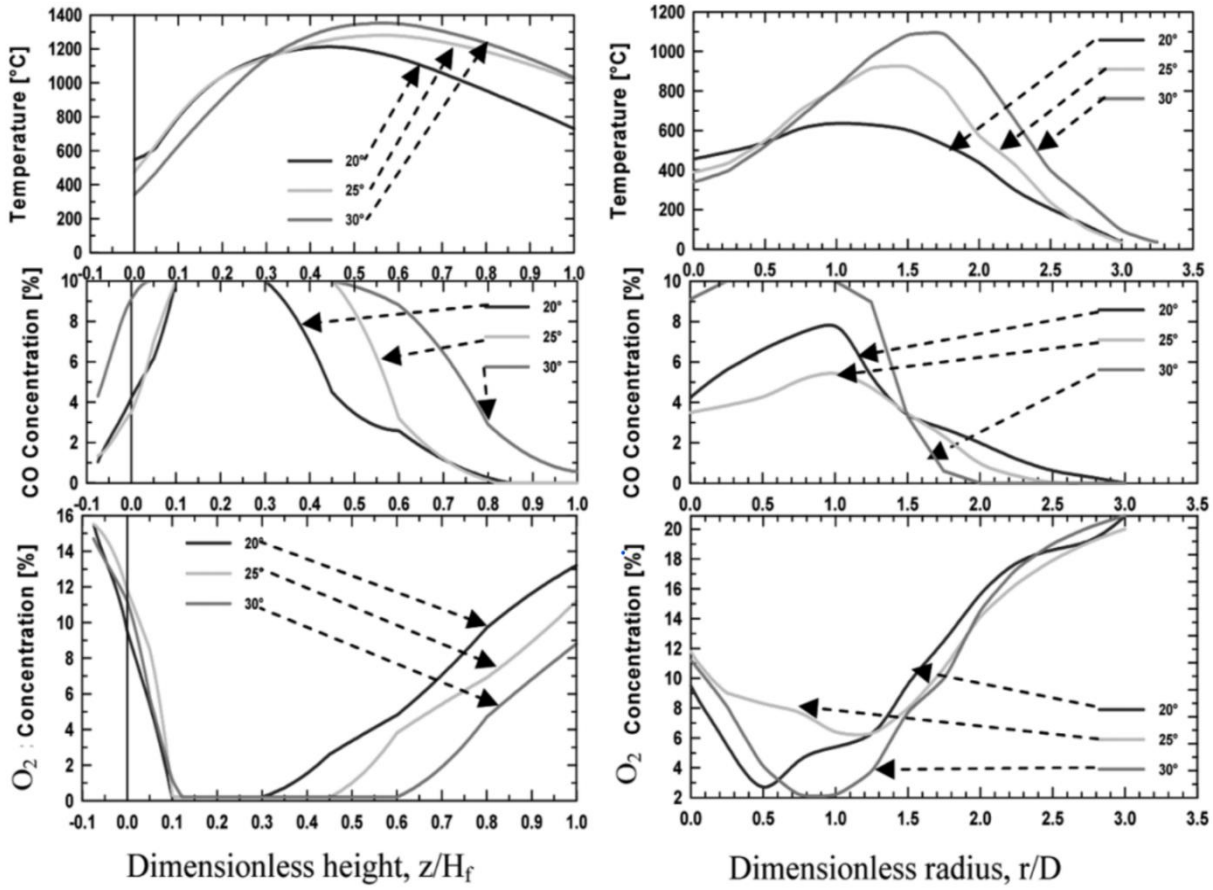

Figure 17: Profiles of oxygen concentration, CO_2 Concentration, and temperature along radial and axial directions

figure 17, the graphs that represent the lower limit of blowout at all LD are on the left while those that represent the upper limit of blowout are on the right. The gap between the lower and upper limits of extinction represents the region of stability. The scatter in figure 18 shows that increasing the air co-flow velocity widens the flame stability region. So, the most important conclusion is that increasing the co-flow velocity results in increasing the stability limits. The lower flame extinction limit was not improved as much as the upper limit, as the upper limit curves are more shifted outwards in comparison to the lower limit curves. Also, smaller stable flame region is noticed at high jet Reynolds number which points out that there is a critical point above which the blowout occurs. The decrease in this stability region is because of the high turbulence effect that occurs at high jet Reynolds number [6].

To study the structure of the flow field to address how the air co-flow enhances stability, Elbaz et al. [6] created diagrams showing the velocity vectors variation vertically along the axial direction and radially outward from the center of the burner's nozzle. This was done on 0 m/s, 5 m/s, and 10 m/s co-flow velocities with the presence of the cone in all cases to enhance the stability more and more as

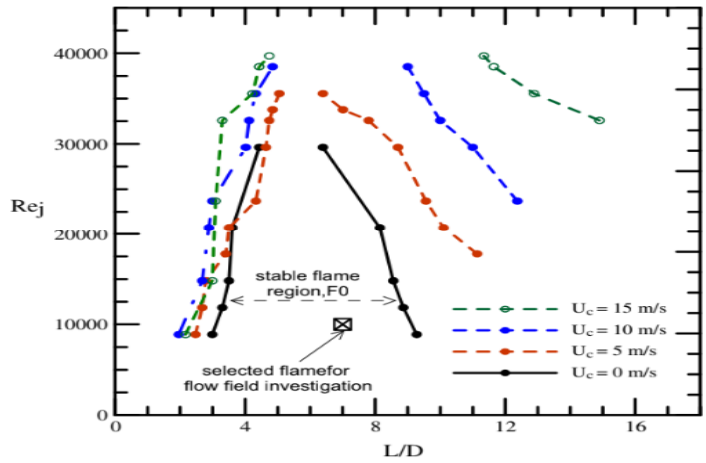

Figure 18: Plot of jet Reynolds number against premixing ratio showing upper and lower flame extinction limits [6]

mentioned previously. The visual observation of the flame under 0 m/s co-flow speed was very consistent with velocity vectors diagram as shown in figure 20, as there is no presence of any recirculation zones which proves the smooth typical profile seen by the observer [6].

The cone attached to the nozzle exit was found to be relatively cold in comparison with the other cases with higher co-flow. This also proves that there isn't any recirculation of hot gases inside the cone.

Increasing the co-flow velocity to 5 m/s and 10 m/s altered the visual appearance of the flame as shown in figure 19. Not only does the flame length decrease, but also the flame width increases upon increasing the co-flow velocities. The flow field structure in figures 21 and 22 is supported by the visual image of the flame. The vectors of velocity at 5 m/s co-flow show the formation of two vortices along the nozzle radius close to the nozzle's rim which widens the flame as shown in figure 21, thus bringing it closer to the nozzle wall. These two vortices happen because of the flux exchange between the co-flow and the flame jet, which further enhances the mixing between fresh fuel-air mixture and the hot byproducts from combustion.

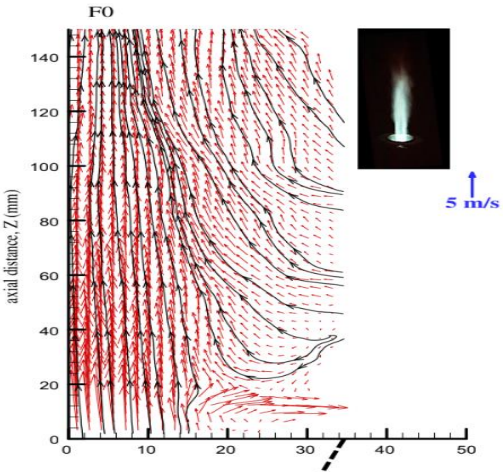

Figure 19: Velocity vectors along axial and radial directions at 0m/s co-flow velocity [6]

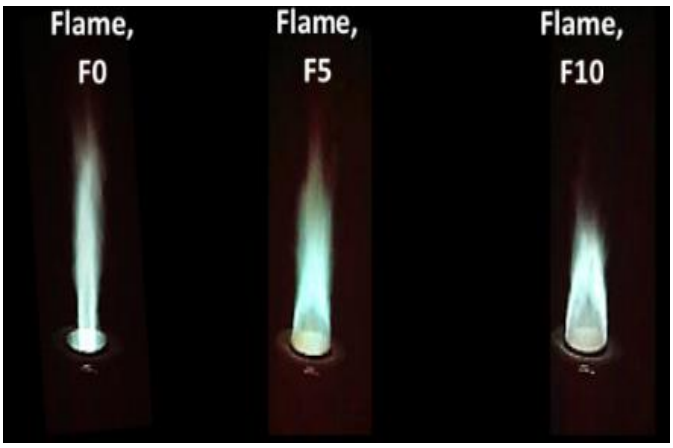

Figure 20: Snap shots of flames at co-flow velocities of 0m/s, 5m/s, 10m/s respectively [6]

This scenario helps in attaching the flame's root to the nozzle region, thus enhancing the region of stability between the lower and upper limit of flame extinction. Adding to this, the velocity vectors seem to shift outward as we move along the axial direction, which make the flame to cease early in height as shown [6].

Further increment up to 10 m/s air co-flow velocity results in the same behavior obtained from 5 m/s co-flow speed as shown in figure 22. But due to higher co-flow velocity, the magnitude of the formed vortices is larger in terms of the size of circulation. Also, the location of the vortices this time is closer to the flame center which further increases the flame stability. Adding to this, having large cortex formation resulted in higher rate of backflow of hot combustion byproducts toward the flame root, leading to higher flame stability [6].

Abdullah et al. [7] tested the stability of biogas in a rectangular slot burner with a nozzle dimension of 100mm by 8mm. The same mechanism of air and bigas flow was done as before as shown in figure 23, where the air leaves from the inner slot and the biogas leaves from the two outer slots so that the flows can start partial premixing in the LD chamber. Five LD chambers were used (LD3, LD5, LD7, LD10, LD16) to

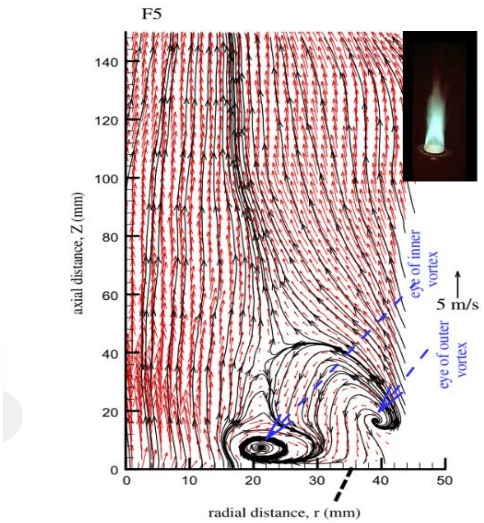

Figure 21: Velocity vectors along axial and radial directions at co-flow velocity 5m/s [6]

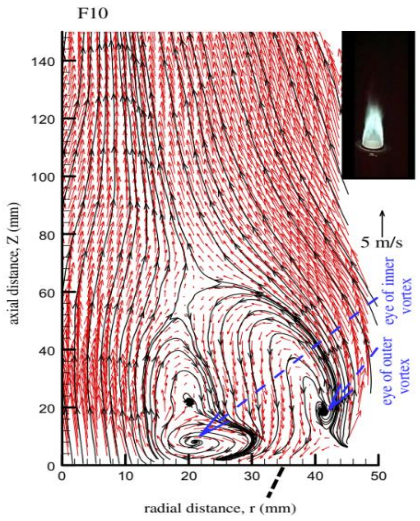

Figure 22: Velocity vectors along axial and radial directions at co-flow velocity 10m/s [6]

investigate the effect of partial premixing length on the stability of flame with biogas as a source of gas supply. Since biogas mainly is nothing but a mixture of methane with CO_2, different mixture proportions between methane and CO_2 were used. He used mixtures of 10%, 20%, 30% CO_2 concentrations out of the total input gas while the rest of the input gas was methane [7].

The results obtained showed that premixing length of LD10 was the best at achieving highest flame stability in all CO_2 mixtures used. Meaning that the highest jet Reynolds number was obtained at flame extinction. While LD3 showed the least stability compared to all other premixing ratios. Because the mixing length in LD3 didn't give enough of the chance of obtaining an inhomogeneous flow which creates rich and lean pockets. Such inhomogeneous flow helps in the formation of multi-reaction zones which helps flame to be more stable under extreme conditions. Also, it was noticed that increasing the CO_2 concentration up to 40% or more resulted in a weaker flame no matter what premixing length was used. As CO_2 concentration increases in the biogas mixture, more methane is needed to account for the heat absorbed by CO_2. The temperature was also measured at the center across the nozzle

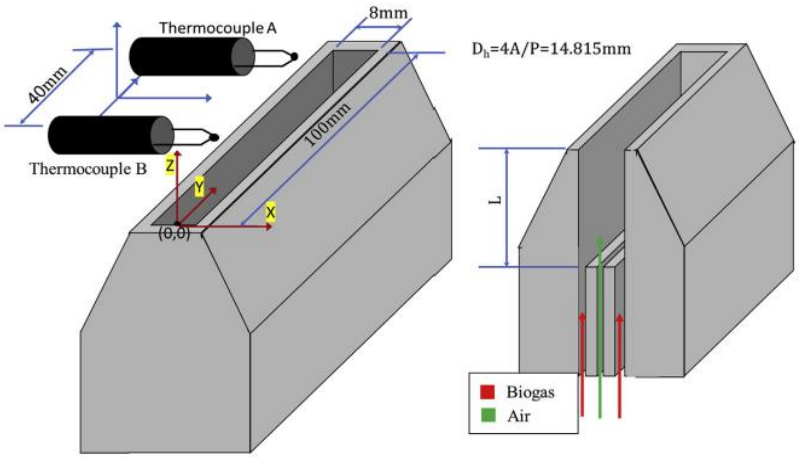

Figure 23: 100mm x 8mm Slot burner with thermocouples mounted on top to measure temperature. Air leaves in the middle slot while biogas leaves at the side slots [7]

exit of 8 mm in thickness along three different vertical positions above the nozzle by a B type thermocouple, to address the effect of increasing CO_2 concentration on the flame temperature. As predicted and shown in figure 24, the temperature profiles at LD10 of all CO_2 concentrations shift down when the CO_2 concentration increases. Because CO_2 acts as a heat sink when increased in concentration, thus decreasing the flame temperature [7].

`In conclusion, the aim of this research is to study the stability of biogas flames in a new slot burner under different levels of mixture inhomogeneity. The effects of CO2 concentration, equivalence ratio, Reynolds number, air to fuel velocity ratio, and air to fuel momentum ratio on the stability and flame structure were investigated.

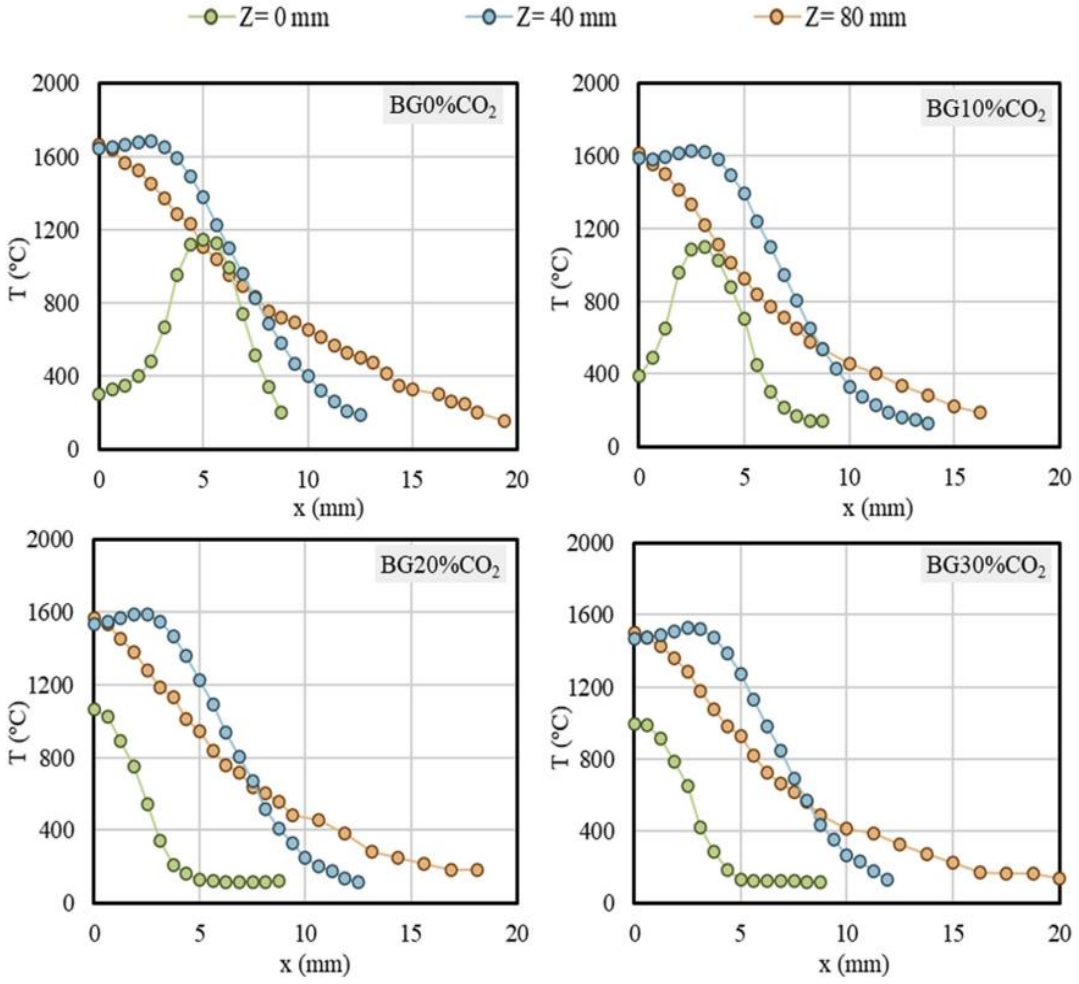

Figure 24: Plots of temperature along radial direction at different height levels made for biogas mixtures with 0%, 10%, 20%, 30% CO_2 Concentrations [7]

Such parameters can greatly affect flame stability characteristics and open the window for more inventions to be made. Velocity and momentum ratios can be increased and decreased by increasing the slot dimensions compared to slots used before. At the same time, exchanging the exits of air and biogas mixture flows with each other will help in achieving a different range of velocity ratios that need to be explored. So, air instead can flow through the two external slots while the biogas is to flow in the middle slot, and this is the opposite of figure 23. Patterns of Reynolds number against velocity and momentum ratios were created to address the conditions at which the flame will be more stable.

Chapter 3

Experimental

3.1 Experimental Setup

The employed burner design has a rectangular slot shape of 60 mm x 10 mm where air travels in the two external slots and fuel travels in the middle slot as shown in the schematic burner exit view in figure 25. All slots have same length of 60 mm, but the slot widths are different. Both air slots have widths of 1 mm while the single middle slot width used for fuel is 6 mm. The longitudinal cross-section of the burner in figure 25 shows that air enters from both sides of the burner while fuel enters from bottom chamber in the burner and then flows up to the burner exit. In previous research work, the opposite was done as fuel was used to flow in the two external slots while air flows in the middle. The current scenario was done to achieve different flow velocities and examine different flow areas on the mixing field.

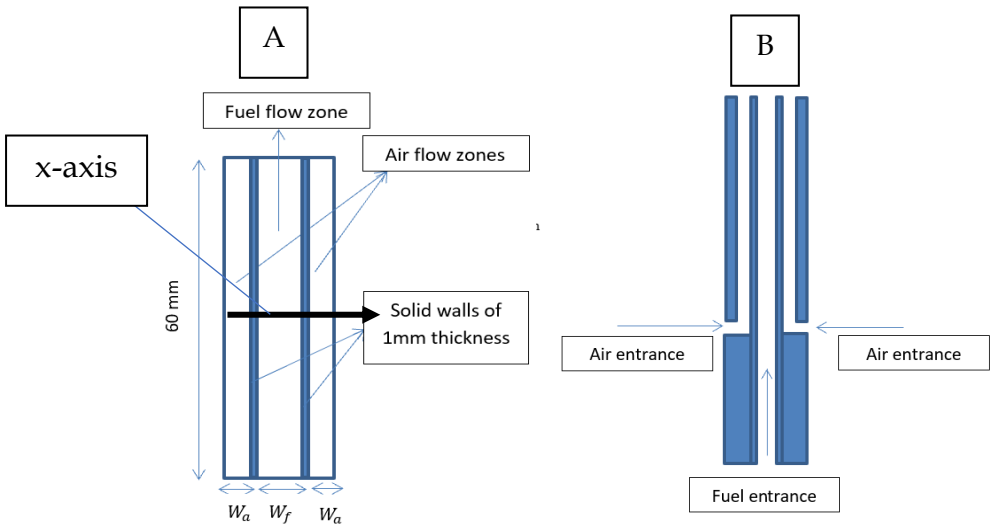

Figure 25: Schematic diagram showing burner (A) top view and (B) longitudinal section view

As shown in figure 26, there are two side chambers responsible for receiving

air from the source and letting it flow through side slots. The two lower connected chambers receive the biogas mixture from the source allowing it to flow in the middle slot without being mixed with air yet. The fuel chambers are designed with guiding sheets as shown in figure 26 to allow more flow regulation, thus avoiding spontaneous flow irregularities. A hollow chamber of 60 mm by 10 mm inner dimensions is mounted on top of the burner exit to allow air and biogas to mix for some length called premixing ratio (LD) as shown in figure 26. Several hollow chambers with different LD were used to investigate the effect of different partial premixing lengths on biogas-air mixture flame stability. The LDs used are 1, 3, 5, 7, 9, 12, and 15.

A Blower was connected at the beginning of the tunnel below while the burner was mounted on the tunnel exit to supply air co-flow with different velocities. To have regular supply of air co-flow, honeycomb and several mesh sheets were placed in between the blower and the burner. As mentioned earlier, air co-flow makes the flame more stable because it supplies the flame from both sides with small vortices that act

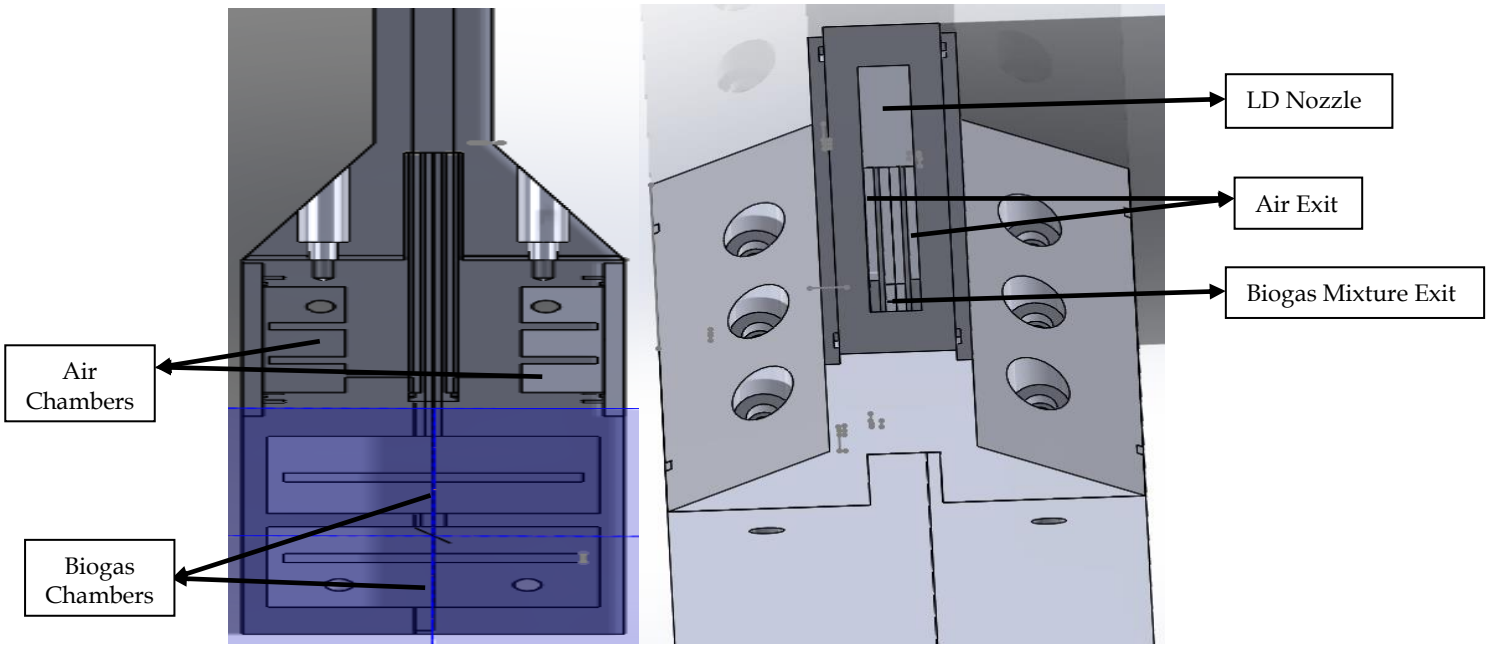

Figure 26: Longitudinal section view and top view of the burner in Solid Works

as anchors thus bonding the flame with the burner nozzle exit. Accordingly, co-flow velocities of 5 m/s, and 10 m/s were applied on LD5 to investigate the effect on air-biogas mixture.

The biogas mixture was achieved by mixing natural gas (containing 96% - 99.4% methane) from the source with CO_2 supplied by the cylinder. Different CO_2 concentrations of 0%, 10%, 20%, 30%, and 40% were prepared prior to entering the burner. To control the volume flow rate of NG and CO_2 lines, both flows were not mixed before passing by the needle valves and sensors to assure the needed constituents of biogas are achieved as shown in figure 27. Four main lines of NG and two main lines if air present in the lab were directly connected to the control unit along with the single line coming from the CO_2 cylinder. Inside the control unit there are valves and sensors to control and read the flow rate. By using several Y-connections between the hoses of the four NG lines and the CO_2 line, these five lines were mixed and supplied as another four lines containing biogas mixture as shown in figure 27. Air lines were divided into another four lines because the burner's air chamber has four inlets, and to allow for more air flow regulation.

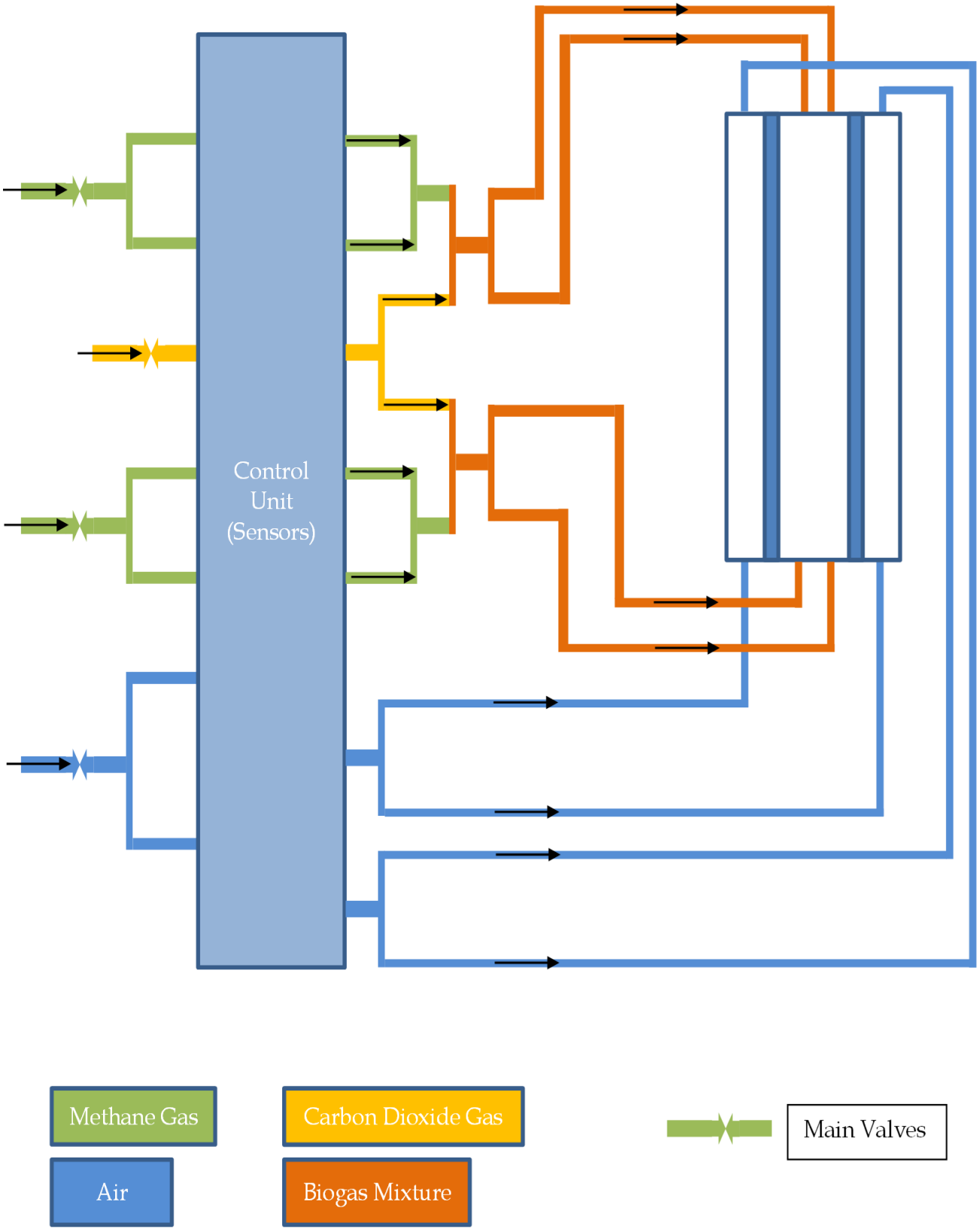

Figure 27: Schematic diagram for the lines entering and leaving the control unit

There were two types of volume flow meters used to measure the flow of air, CO_2, and NG. Honeywell HAF300slm sensors were used for air and CO_2 lines (accuracy of +/- 0.5% at 0%-14% of full scale and +/- 3.5% at 14%-100% of full scale). Sensirion SFM3000 sensors were used for the four NG lines having higher accuracy of +/- 0.05% of the full scale. Arduino-uno was used inside the control unit to gather the signals from all sensors, which was later connected to the laptop. By applying a code including formulas on Arduino software, the excel file was able to display the flow rates by all the lines, and most importantly Reynolds number and equivalence ratio at any instant.

The temperature of the flame was also measured by scanning the flame with a B-type thermocouple. With the help of the 3D mechanism shown in figure 28, the thermocouple was moved by steps of 0.5 mm along the slot width of 10mm, and all readings were taken at middle of the slot's length (along x-axis in figure 25). The B-type thermocouple wires are made of platinum with 30% Rhodium as a positive terminal and platinum with 6% Rhodium as a negative terminal. Both terminals are connected at a junction of 300 micro-meter in size. To capture the temperature reading, Multimeter (accuracy of +/- 0.01 mV) was connected at both terminals of the thermocouple from the other end of the junction. Readings on Avometer were fluctuating so the average of the first 5 readings were calculated to be the temperature at a point.

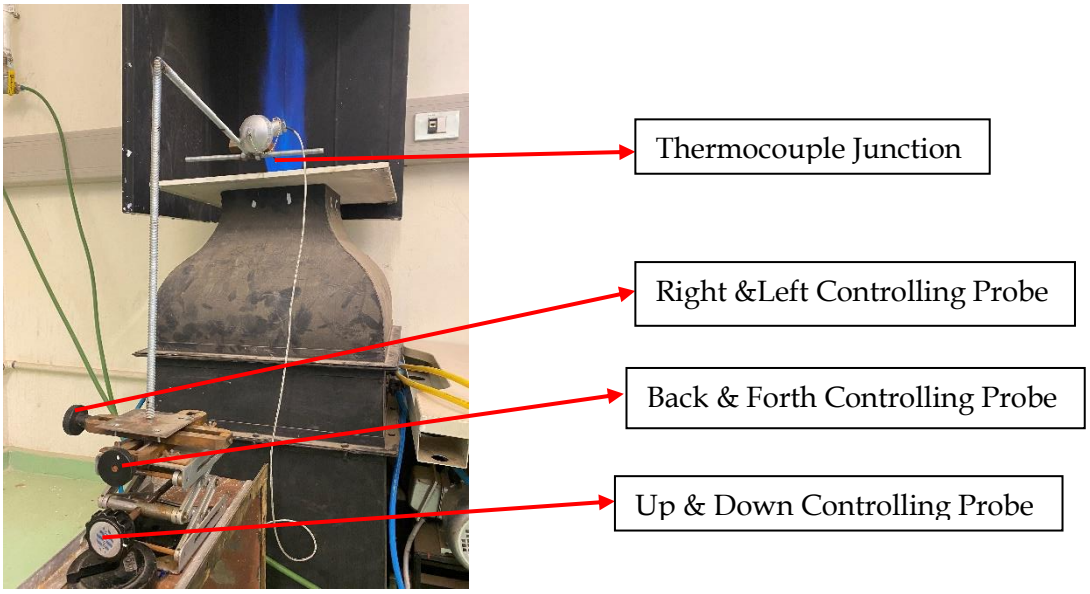

Figure 28: 3D Mechanism Holding Thermocouple during Flame Operation

3.2 Experimental Technique

A series of steps were taken to investigate how the flame stability is affected by changing CO_2 concentrations, mixing lengths, air co-flow velocities. In this research the parameters which indicate flame stability are Reynolds number, equivalence ratio, and fuel to air velocity ratio. The experiment starts by mounting any LD part on the burner's nozzle and then start adjusting the NG and CO_2 flow rates via the needle valves accordingly without allowing air to flow into the burner. The biogas mixture flow rate is varied from 10 slm up to 60 slm (with steps of 10 slm) for a fixed CO_2 concentration, and the corresponding Reynolds number, equivalence ratio, and velocity ratio are recorded for each biogas flow rate at flame extinction as shown in table 6. For instance, if it is required to have biogas mixture for 20 slm at 10% CO_2 concentration as a flow rate, then the NG flow rate need to be adjusted at 18 slm and CO_2 at 2 slm. Flame extinction is achieved by increasing the air flow rate through the use of needle valves mounted on the two air-lines entering the control unit. Table 6 should be done and filled for other CO_2 concentrations as well which are 20%, 30%, and 40% of the total biogas mixture. This whole process was repeated for other LDs to see the relation between partial premixing length and biogas flame stability.

Table 6: Natural gas and CO_2 flow rates at each required biogas mixture

Biogas Flow Rates (m^3/s)	NG 4 Lines Flow rates (slm)				Total NG Flow Rate (90%)	Q_C02 (10%) (slm)	Air Lines flow rate		Reynolds No.	Equivalence Ratio	Velocity Ratio
	Q_NG,1	Q_NG,2	Q_NG,3	Q_NG,4			Q_air,1 (slm)	Q_air,2 (slm)			
10	2.25	2.25	2.25	2.25	9	1	**Air Flow Increased Gradually & Recorded at Flame Extinction**		**Recorded at Flame Extinction**		
20	4.5	4.5	4.5	4.5	18	2					
30	6.75	6.75	6.75	6.75	27	3					
40	9	9	9	9	36	4					
50	11.25	11.25	11.25	11.25	45	5					
60	13.5	13.5	13.5	13.5	54	6					

To study the effect of different CO_2 concentrations contained in biogas mixture on flame temperature, a B-type thermocouple was used to scan the flame temperature at 3 vertical levels above the burner nozzle. The scan was performed above the LD7 and LD15 nozzle by 5 mm, 30 mm, and 60 mm for all CO_2 concentrations, and under fixed flame parameters of 1.5 equivalence ratio and turbulent flame with Reynolds number of 3500. Flames with all CO_2 concentrations were adjusted to have at the end same Reynolds number and equivalence ratio to clearly study the effect of CO_2 alone on flame temperature.

3.3 Calculations

The sensors used to measure the flow rates send signals to the Arduino with flow rates values so that these values be processed by a series of equations. The main aim is to calculate the equivalence ratio, Reynolds number, velocity ratio, and momentum ratio out from the flow rates measured. These parameters help in analyzing the flow conditions at the blowout.

The mole fraction of CO_2 and methane are calculated out of the total biogas amount by dividing each of the components flow rate by the total flow rate of biogas as shown in equation 1 and 2.

$$X_{CO_2} = \frac{Q_{CO_2}}{Q_{CO_2} + Q_{CH4}} \quad (1)$$

$$X_{CH4} = 1 - X_{CO_2} \quad (2)$$

Also based on the flow rates measured, mass flow rates of methane, CO_2, and air can be calculated. This is done by using ideal gas law to calculate density of each flow (as shown in part 3) which will later be multiplied by the corresponding flow rates to calculate mass flow rate of each flow separately (as shown in part 4).

$$\rho_{air} = \frac{P_{atm} * M_{air}}{R * T} \qquad \rho_{CH4} = \frac{P_{atm} * M_{CH4}}{R * T} \qquad \rho_{CO_2} = \frac{P_{atm} * M_{CO_2}}{R * T} \tag{3}$$

$$m°_{air} = \rho_{air} * Q_{air} \qquad m°_{CH4} = \rho_{CH4} * Q_{CH4} \qquad m°_{CO_2} = \rho_{CO_2} * Q_{CO_2} \tag{4}$$

After calculating the mass flow rates, the actual air to fuel ratio can now be calculated by dividing the mass flow rate of air by the mass flow rates of methane and CO_2 as shown in equation 5. Equation 6 shows how the stoichiometric air to fuel ratio is calculated. This equation is derived from the combustion formula of biogas mixture. Mole fractions and molecular masses of methane and CO_2 are needed to calculate the stoichiometric air to fuel ratio as shown in equation 6.

$$A/F_{actual} = \frac{m°_{air}}{m°_{CH4} + m°_{CO_2}} \tag{5}$$

$$A/F_{Stoichiometric} = \frac{2 * (1 - X_{CO_2}) * 32 * \frac{1000}{233}}{(1 - X_{CO_2}) * M_{CH4} + X_{CO_2} * M_{CO_2}} \tag{6}$$

Equivalence ratio now can be calculated by dividing the stoichiometric air to fuel ratio by the actual air to fuel ratio as shown below.

$$\Phi = \frac{\mathbf{A/F_{St.}}}{\mathbf{A/F_{Actual}}} \tag{7}$$

A series of equations need to be done before calculating the Reynolds Number. First the air mole fraction is calculated by dividing the air flow rate by the total flow rate of methane, CO_2, and air as shown in equation 8. Then the fuel or biogas density is calculated using methane and CO_2 densities and mole fractions as shown in equation 9. Now the density of the mixture consisting of air, methane, and CO_2 can be calculated by using the previously obtained fuel density and air mole fraction.

$$X_{air} = \frac{Q_{air}}{Q_{air} + Q_{CH4} + Q_{CO_2}} \tag{8}$$

$$\rho_{fuel} = X_{CH4} * \rho_{CH4} + X_{CO_2} * \rho_{CO_2} \tag{9}$$

$$\rho_{mix} = X_{air} * \rho_{air} + (1 - X_{air}) * \rho_{fuel} \tag{10}$$

To find the mixture velocity, the mass flow rate of the whole mixture is needed by summing up air, methane, and CO_2 flow rates together as shown in equation 11. Mixture's velocity can now be calculated by dividing the mixture's mass flow rate by the product of the mixture's density and the nozzle area as shown in equation 12.

$$\mathrm{m^{\circ}_{mix}} = \mathrm{m^{\circ}_{air}} + \mathrm{m^{\circ}_{CH4}} + \mathrm{m^{\circ}}_{CO_2} \quad (11)$$

$$\mathrm{U_{mix}} = \frac{\mathrm{m^{\circ}_{mix}}}{\rho_{\mathrm{mix}} * (\mathrm{L} * \mathrm{W})} \quad (12)$$

To calculate the dynamic viscosity of the mixture, the air mass fraction is found first by dividing the air mass flow rate by the mixture flow rate as shown in equation 13. Mixture's dynamic viscosity is calculated by using air mass fraction, CO_2 mole fraction, and the dynamic viscosities of air, methane, and CO_2 as shown in equation 14.

$$\mathrm{Y_{air}} = \frac{\mathrm{m^{\circ}_{air}}}{\mathrm{m^{\circ}_{mix}}} \quad (13)$$

$$\mu_{\mathrm{mix}} = \mathrm{Y_{air}} * \mu_{\mathrm{air}} + (1 - \mathrm{Y_{air}}) * \left(\left(1 - \mathrm{X}_{CO_2}\right) * \mu_{\mathrm{CH4}} + \mathrm{X}_{CO_2} * \mu_{CO_2} \right) \quad (14)$$

The last parameter needed before calculating Reynolds number is the hydraulic diameter of the burner's nozzle. Then Reynolds number is calculated by dividing the product of mixture's density, mixture's velocity, and hydraulic diameter by the mixture's dynamic viscosity as shown in equation 16.

$$\mathrm{D_h} = \frac{4 * \mathrm{L} * \mathrm{W}}{2 * (\mathrm{L} + \mathrm{W})} \quad (15)$$

$$\mathrm{Re} = \frac{\boldsymbol{\rho_{mix} * U_{mix} * D_h}}{\boldsymbol{\mu_{mix}}} \quad (16)$$

The air to fuel velocity ratio is very important to find as it gives a strong indication about the best mixing conditions that achieve the highest Reynolds number. Simply, it is calculated by dividing air flow velocity by the velocity of biogas. The

velocity of each gas can be substituted by the ratio of volume flow rate by the gas exit area as shown in equation 17.

$$V_r = \frac{U_{air}}{U_{fuel}} = \frac{\frac{Q_{air}}{2*L*W_{air}}}{\frac{Q_{CH4}+Q_{CO_2}}{L*W_{fuel}}} \quad (17)$$

The last important parameter that needs to be found is the air to fuel momentum ratio. This parameter gives also an insight into the best mixing conditions that achieves highest Reynolds Number.

$$I = \frac{A/F_{st.}*V_r}{\Phi} \quad (18)$$

Chapter 4

Results and Discussion

4.1 Effect of Premixing Ratio on Combustion Characteristics of Biogas

The results truly showed the behavior of flame stability under different partial premixing lengths. In this research, air was allowed to flow in the outer slots of 1 mm thickness while the biogas mixture was allowed to flow in the inner slot of 6 mm thickness in contrary to previous research work. This was done to achieve a wider range of air and biogas flow velocities. Values of methane, CO_2, and air flow rates were measured at flame blowout by the sensors in standard liter per minute to be able to calculate main parameters like; Reynolds number, equivalence ratio, air to fuel velocity ratio, and air to fuel momentum ratio. These parameters are calculated using equations 7, 16, 17, and 18. Flame blowout was achieved by increasing the air flow rate at fixed fuel flow rates of 10, 20, 30, 40, and 60 standard liters per minute, and then Reynolds number and equivalence ratio were recorded accordingly. Stability plots can now be plotted by having Reynolds number on the y-axis and equivalence ratio on x-axis. These plots indicate the value of Reynolds number (ratio of inertial to viscous forces) at the blowout and its corresponding equivalence ratio (ratio of actual air to fuel ratio to stoichiometric or ideal air to fuel ratio). Such plots are very important as any point below the scatter means that the flame is stable and will not blow out and vice versa. It was noticed from the stability patterns in figure 29, that the highest flame stability reached under absence of CO_2 was achieved by using several premixing ratios starting by 15, 9, 5, 7, and 12 respectively. Poorest stability was noticed at LD1 and then LD3. This is due to being very close to the non-premixed conditions, as LD1

and LD3 are short hollow slots which allow little or no partial premixing before flame ignition. In comparison to previous research work [7], the results are promising because higher Reynolds Numbers were achieved at lower equivalence ratios. As shown in figure 29, the highest Reynolds Number of 17,000 and equivalence ratio of 1.23 was achieved at LD9, and Reynolds Numbers above 15,000 at equivalence ratios lower than 1.33 were also achieved at LD 5, 7, and 15. On the other hand, lower Reynolds Numbers below 5000 were achieved at very high equivalence ratios up to 5.1 when using LD = 1, indicating less efficiency and stability. Such scenario indicates that more fuel is needed to just increase the Reynolds number by small amounts, which is because of the poor mixing conditions between fuel and air. Same results were also achieved by Baudoin et al. [20], as it was concluded that there is an optimal level of partial premixing at which the flame is most stable. This evidence was achieved by using a concentric burner with two concentric tubes for air and methane [20], and the mixing length was varied by controlling the tube positions. Same results were also obtained through using perforated burner for methane-air mixtures by

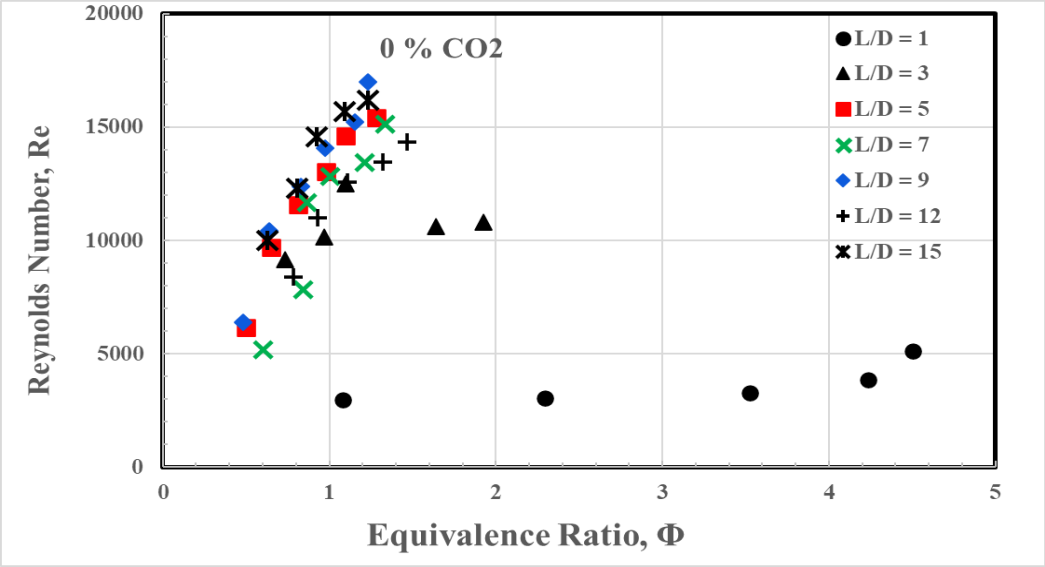

Figure 29: Plot of Reynolds number against equivalence ratio at 0% CO_2 concentration for all premixing ratios

Rashwan et al. [21]. A wider range of flammability limits was obtained at a certain level of premixing length, showing that high flame stability can be obtained at partial premixing conditions.

Regarding the biogas mixture with 10% CO_2 concentration, LD5 achieved the highest operating conditions at flame extinction this time compared to other premixing ratios. In this premixing ratio, the equivalence ratio ranged from 0.55 up to 1.17 while Reynolds Number ranged from 5407 to a maximum value of 16,867. The next following premixing ratios with high stability curves and better parameters at extinction were at LD = 15, 12, 7, and 9 respectively. The order of stability in all premixing ratios under 10% CO_2 concentrations mentioned above was also maintained for the rest of CO_2 concentrations 20%, 30%, and 40% as shown in figure 30. However, as the CO_2 concentration increases the range of operation for Reynolds number and equivalence ratio decrease. Premixing ratio of 15 proved to be the best in flame extinction operating parameters in the absence of CO_2, but when supplying some CO_2 in biogas mixture, the premixing ratio of 5 showed best performance for all possible CO_2 concentrations. This difference in order of stability happened because the arrangement of rich and lean pockets was altered just by the introduction of CO_2 into the mixture.

Premixing ratio of 1 possessed the same pattern in Reynolds versus equivalence ratio graphs under all CO_2 concentrations, as it showed the least slope ever in figure 30. Not only the poor mixing in LD1 resulted in fewer lean and rich pockets of biogas during the flow, but also the presence of CO_2 gas inside biogas mixture leads to a cooling effect of the biogas-air mixture. So, more methane is needed when CO_2

concentration increases to compensate for the heat absorbed by CO_2 and supply the mixture with activation energy to stabilize the flame more. Also, stable flames were created at lower Reynolds Number values, as CO_2 lowers the flame speed. The presence of CO_2 in biogas and oxygen in air increases the competition on hydrogen atoms, which may result in the formation of CO due to the CO_2 reaction with H. Such products decrease the flame temperature thus affecting the flame extinction operating parameters. It is also noticed that at higher CO_2 concentrations the slope of the graph in LD1 decreases, thus reaching higher equivalence ratios up to 8.28 while applying 40% CO_2 concentration.

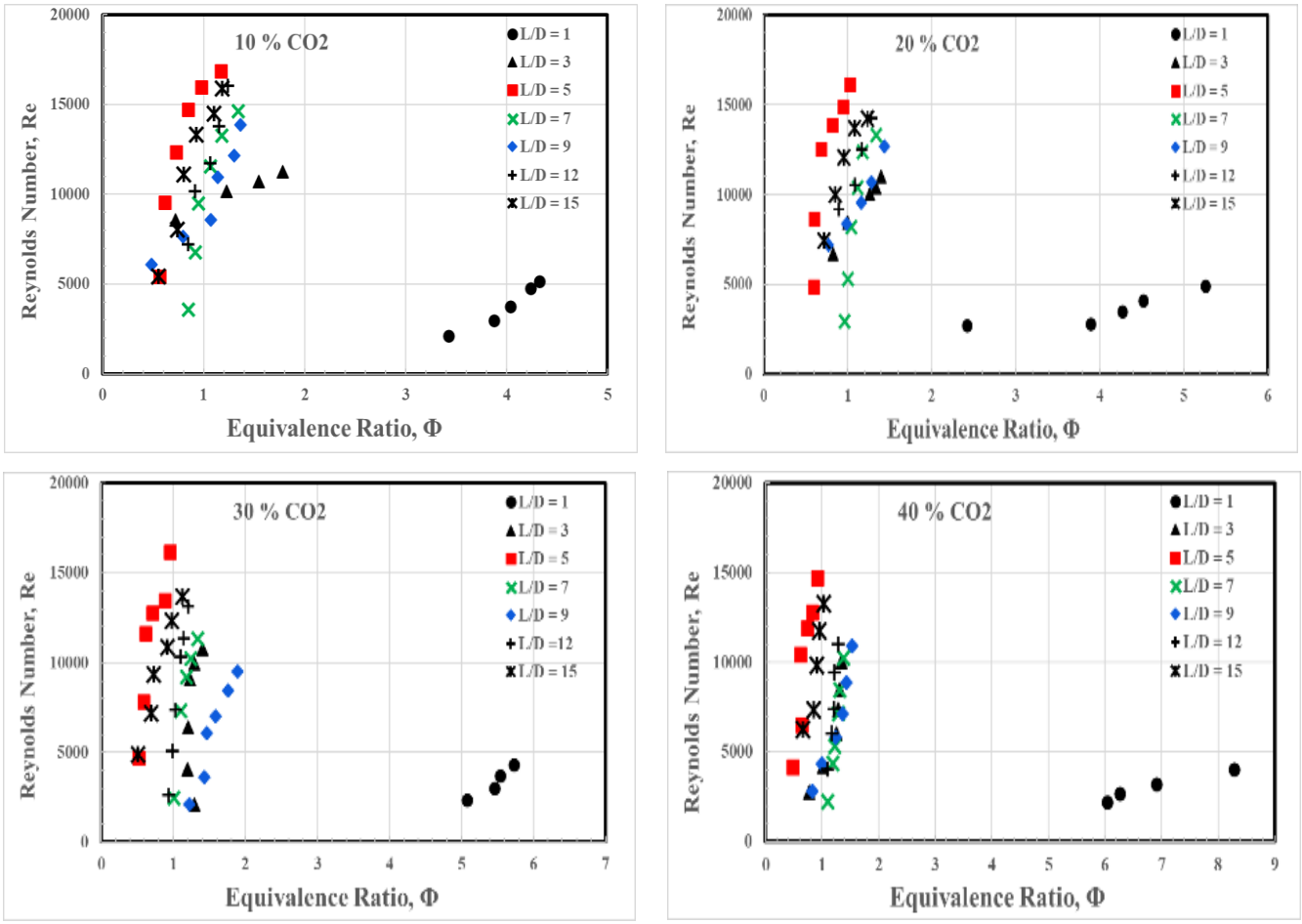

Figure 30: Reynolds against equivalence ratio for all premixing ratios at 10%, 20%, 30%, 40% CO_2 concentrations

4.2 Effect of CO_2 Concentration on Combustion Characteristics

CO_2concentrations of 10%, 20%, 30%, and 40% of the total fuel supply were implemented by controlling the supply valves of methane and CO_2. Air flow rate increased gradually till flame blowout at fixed biogas mixture flow rates of 10, 20, 30, 40, 50, and 60 standard liter per minute, and again Reynolds number and the equivalence ratio were recorded on the spot. The effect of increasing CO_2 concentration was obvious when stability curves at different CO_2 concentrations are all plotted at a fixed premixing ratio values. As predicted, the scatter plot at LD1, LD7, LD12, and LD15 becomes less steep by increasing the concentration of CO_2 in biogas mixture as shown in figure 31. This indicates that the presence of CO_2 decreased the endurance of flame against flow rates with high Reynolds numbers that was obtained before when CO_2 was absent. Same investigations were done by Liu et al. [22] through using a circular burner which creates a partially premixed air-biogas mixture inside a cup which is later ignited. The obtained results showed that CO_2 contained in biogas not only reduces the reaction rate, but it also strongly dilutes the whole mixture during combustion. As a result, a lower flame temperature at combustor exit was reached in comparison to natural gas combustion. Ghenai et al. [23] measured the peak flame temperature for biogas coming from two sources which are landfill and anaerobic digester. It was found that peak flame temperature decreased by 37% and 22% in comparison to natural gas flame temperature for both landfill biogas and anaerobic digester biogas respectively. Besides, the gaps between the scatter points at all CO_2 concentrations get closer to each other when the premixing ratio increases. Premixing ratio of 15 represents almost fully premixed conditions at which the flame becomes

also more stable, but not as higher stability as in premixing ratio of 5 where partial premixing occurs.

As mentioned previously, that premixing ratio of 5 achieved highest operating parameters at flame extinction for all CO_2 concentrations. In the laminar part of 0% CO_2 concentration, the flame attained highest operating parameters at flame extinction in comparison to 10%, 20%, 30% and 40% CO_2 concentrations as shown in figure 32. However, in the turbulent part the stability pattern for 10%, 20%, 30%, and 40% CO_2 concentrations became slightly higher than using pure methane with 0% CO_2. Such findings are great because higher stability at LD5 can be achieved for biogas mixtures with high CO_2 concentrations, which compensates the negative effects of

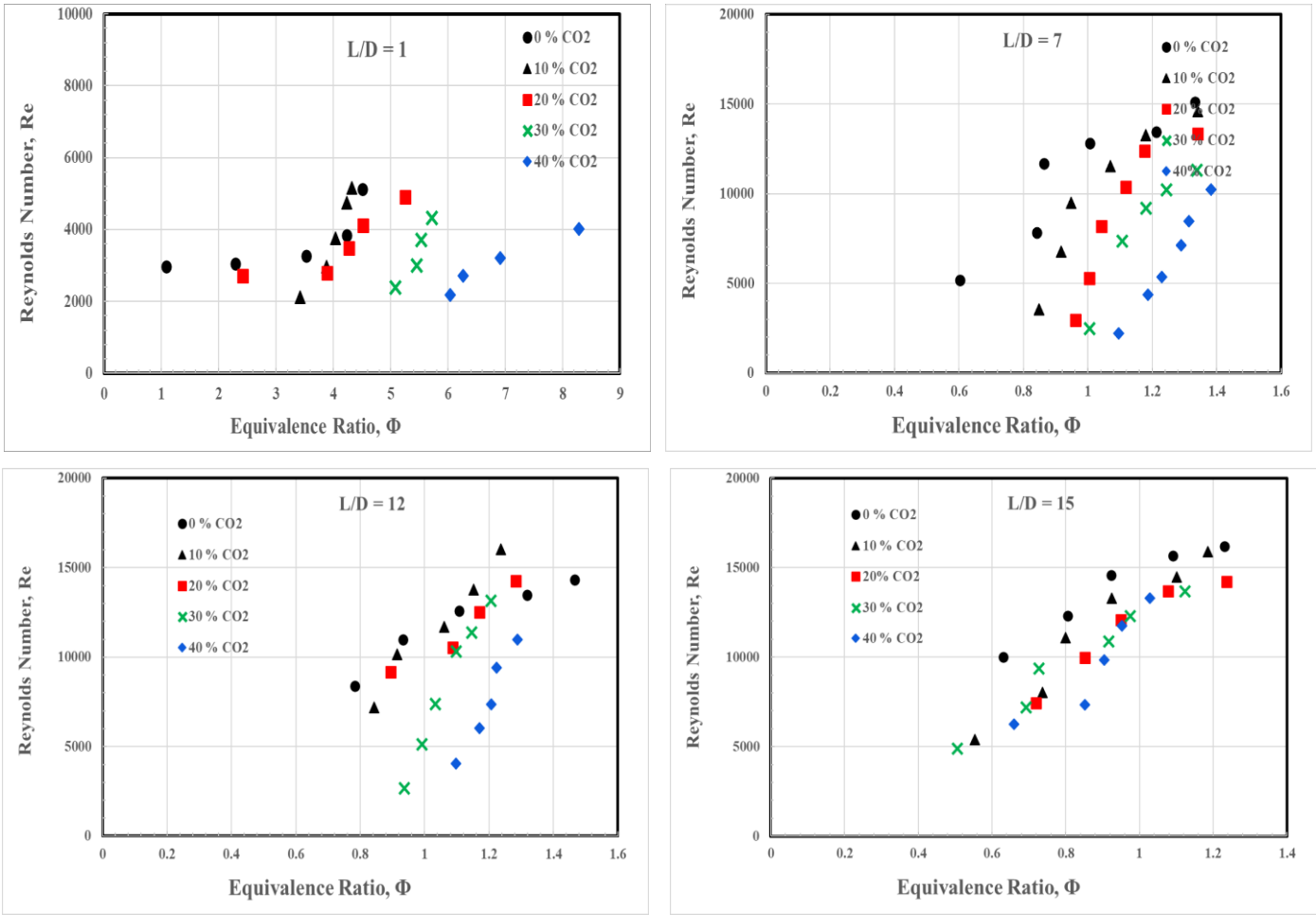

Figure 31: Reynolds against equivalence ratio for all CO_2 concentrations at premixing ratios 1, 7, 12, 15

CO_2 on laminar burning velocity and adiabatic flame temperature. At this partial premixing level, a high level of inhomogeneous mixing is established thus creating lean and rich pockets throughout the flow. These multi-reaction zones in the flow have an essential role in preventing local extinction.

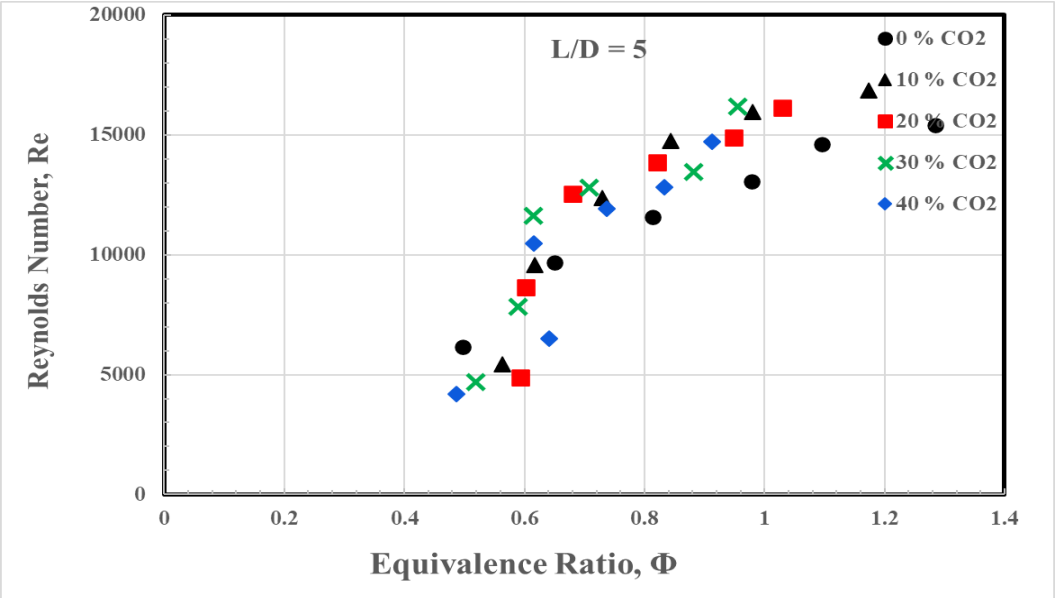

Figure 32: plot of Reynolds number against equivalence ratio at all CO_2 concentrations for premixing ratio 5

4.3 Velocity Ratio Effect on Flame Stability

Velocity ratio is the ratio of air flow velocity to biogas mixture velocity, so of course it plays an essential role in controlling the mixing field thus affecting the flame extinction operating parameters. Plots of Reynolds versus velocity ratio were done to clearly study the effect of different premixing ratios on flame stability. It is clearly noticed from figure 33 that maximum Reynolds Number of the flow which indicates higher flame stability, is always and almost achieved at the mid-range of the velocity ratio values. Such findings indicate that a specific level of partial premixing between biogas and air is required to achieve higher flame stability. Increasing CO_2 concentrations in biogas mixture increased the gaps between the patterns as shown in figure 33, and this is because at higher CO_2 concentrations the Reynolds Number of all scatters points has decreased thus widening the gaps between the scatters. The patterns of all cases show that there is an inverse relation between Reynolds Number and velocity ratio, since increasing the air flow velocity with respect to biogas mixture helps in deteriorating the flame characteristics by diluting the biogas mixture. This supports the findings by Wang et al. [27], as the stability of flames was deduced by measuring the relative emissions of CH because it indicates the heat release rate qualitatively. The CH regions changed obviously along the radial and vertical axis once the velocities of air and methane increased. A high-speed intensified camera was used to capture the heat release regions which are seen to experience strong oscillations upon the increase of air-methane velocities. Such vibrations deteriorate the heat release regions causing flame extinction at high velocity ratios.

LD1 achieved flame stability at lowest possible velocity ratio in all figures,

indicating that it is almost impossible for air and biogas to partially premix at higher velocities while using very short premixing lengths. At 10%, 20%, 30%, and 40% CO_2 concentrations, LD5 proved to have the highest Reynolds Number across all premixing levels at almost same level of velocity ratios. The next following premixing levels achieving high flame stabilities were 15 and 12. Also, at turbulent conditions LD7 was found to have higher Reynolds Number at flame extinction than LD9, but at laminar conditions the opposite happens.

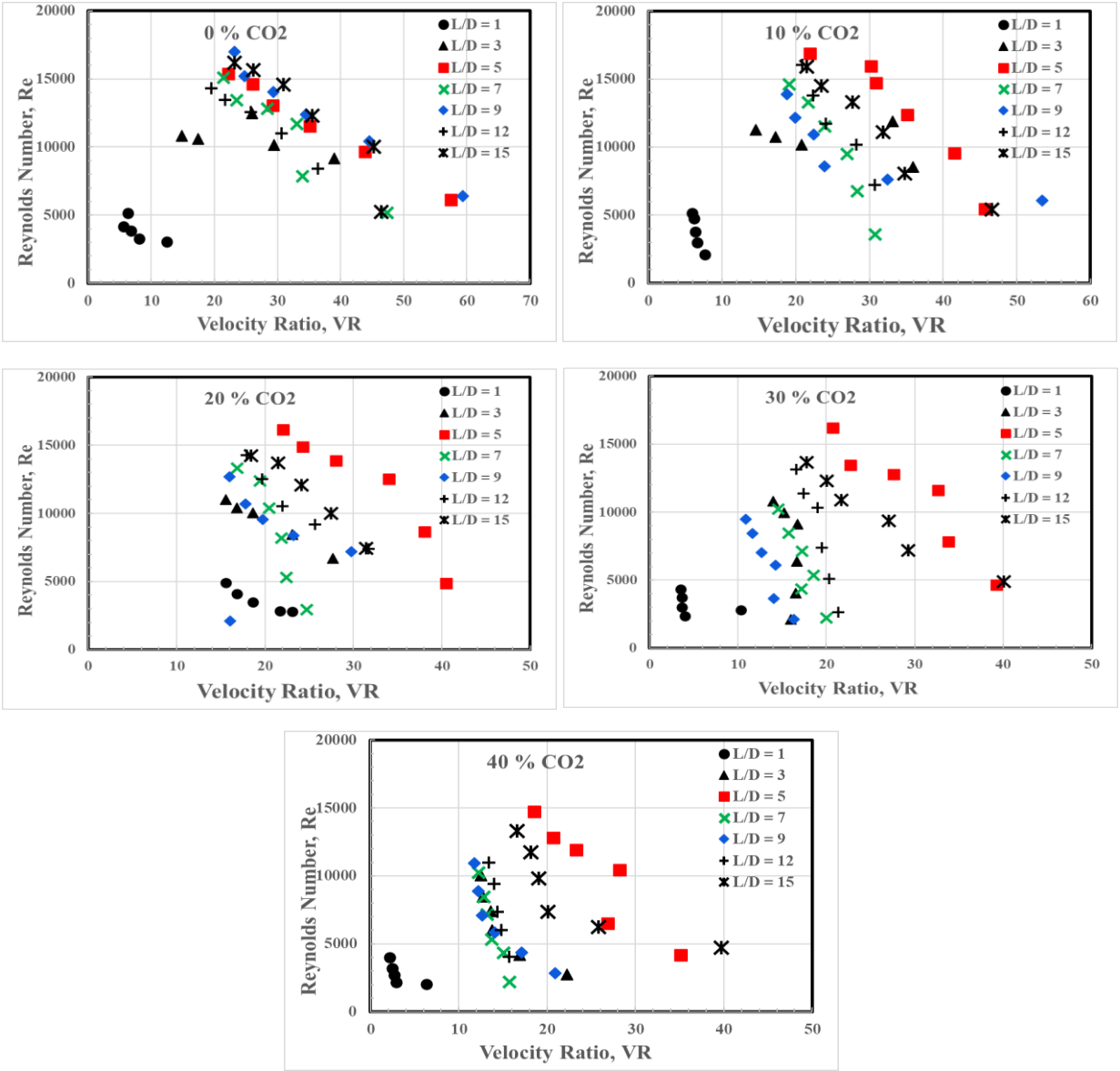

Figure 33: Plots of Reynolds number against velocity ratio for all premixing ratios at 0%, 10%, 20%, 30%, 40% CO_2 concentrations

To study the velocity ratio effect on stability parameters from another perspective, Reynolds Number was calculated by interpolation at fixed velocity ratio values of 15, 20, and 25. This was done to study at which premixing level will the Reynolds number be maximum. Interpolation was done because there are some data points at different fuel flow rates, premixing ratios, and CO_2 concentrations, which didn't achieve exactly a velocity ratio value of 15 or 20 or 25. The three velocity ratios mentioned were chosen because they were located within the scatter points which attained highest Reynolds number in figure 33. Another version of the previous figures was established by creating curves at fixed velocity ratio values instead of premixing ratio levels and changing the x-axis to be premixing ratio levels instead as shown in figures 34. It is clearly observed that there are peaks occurring at specific values of premixing ratios where the flame stability is highest. At 0% CO_2 Concentration, the highest Reynolds number at flame extinction was achieved at LD9 which complies with figure 34. Regarding 10%, 20%, 30%, and 40% CO_2 concentrations, LD5 was found to attain the highest Reynolds Number value in all curves which agree with the scatter plots in figure 32. Also, all curves increase in Reynolds Number gradually beyond premixing ratio of 9 reaching a high Reynolds Number at LD15. Longer hollow chambers having higher premixing ratios can be used in the future to attain higher flame stability.

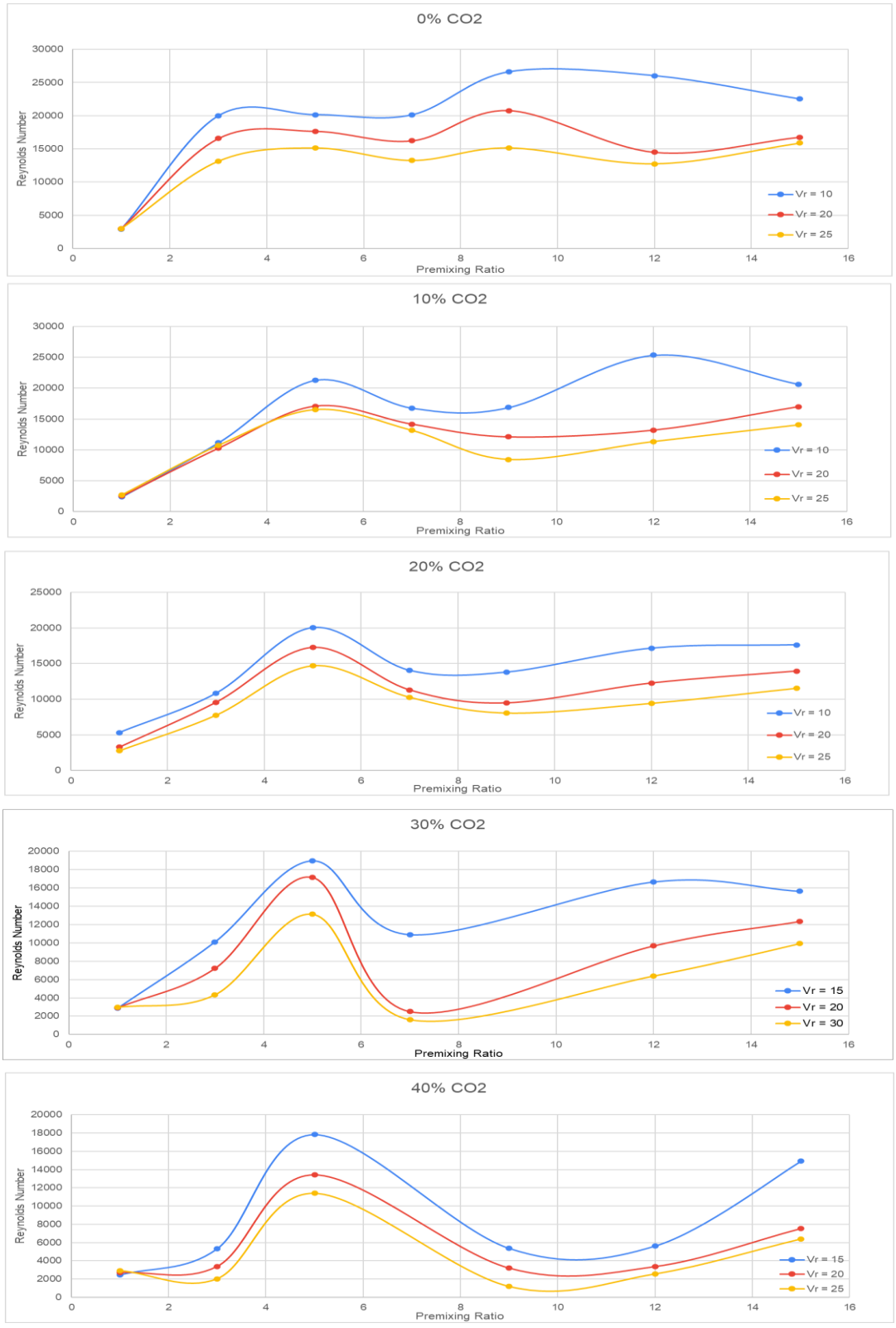

Figure 34: Curves of Reynolds number against premixing ratio at fixed velocity ratio values of 15, 20, 25

4.4 Momentum Ratio Effect on Flame Stability

Momentum Ratio is the ratio between air momentum and biogas momentum, and it does have a great impact on the mixture fraction field. Both momentum and velocity ratios control the mixture fraction field by controlling the distribution of rich and lean pockets throughout the flow which severely affects the flame stability. So, it was found that velocity and momentum ratio possess the same trend against Reynolds number as shown in figure 35. Decreasing momentum ratio means more mixture fraction inhomogeneity and thus having higher gradients in the mixture. This is accompanied by an increase in equivalence ratio, which means that a higher Reynolds Number should be achieved at flame extinction as shown in figure 35. The results support Mansour et al. [17] findings that momentum and velocity ratios affect the segregation of rich and lean pockets within the flow field, thus leading to the inverse proportionality of the mentioned ratios with the equivalence ratio [17]. The same conclusion was also reached by Mastrodonato et al. [28], as the air to fuel jet momentum ratio was studied by using a hydrogen combustion chamber. The decreasing air to fuel momentum ratio not only reduced NOx emissions, but also resulted in more flow inhomogeneity which helped attain enhanced dilution of exhaust recirculated gases with fuel. Such inhomogeneity created rich and lean pockets throughout the flow which in turn enhanced flame stability.

Highest flow Reynolds Numbers were achieved when the flow acquired momentum ratio between 300 to 400 when CO_2 is absent. When the CO_2 concentrations are 10% and 20%, highest Reynolds Numbers were achieved in a momentum ratio range of 150 to 250. The momentum ratio range shifts from 100 to

200 for 30% and 40% CO_2 concentrations. The same premixing ratios Ranking is maintained also in momentum ratio analysis, as LD5 proved to be the best attaining high Reynolds Number at flame extinction (in 10%, 20%, 30%, and 40% CO_2 concentrations at almost same momentum ratio levels) in comparison to all other premixing ratios.

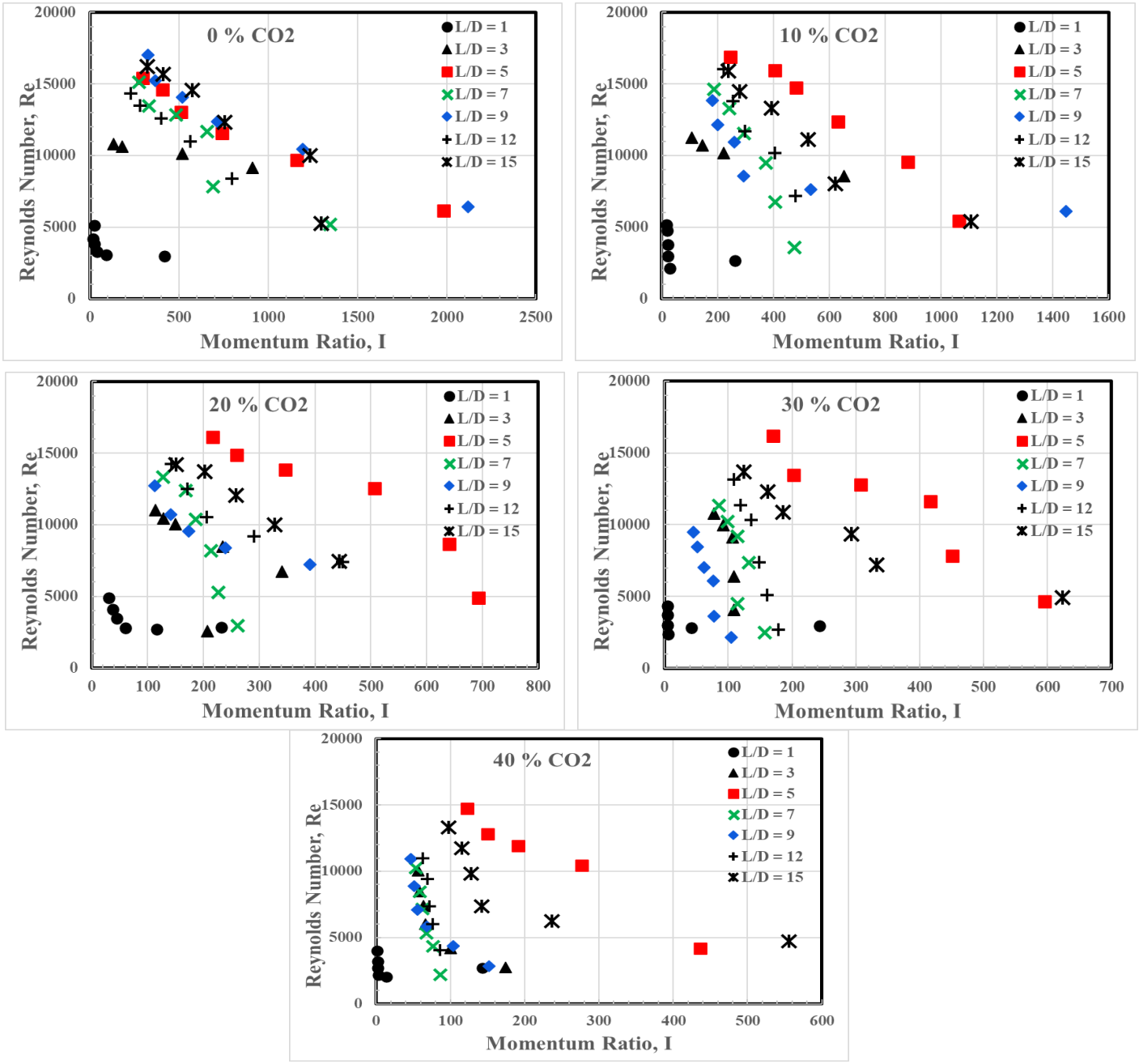

Figure 35: Plots of Reynolds number against momentum ratio for all premixing ratios at 0%, 10%, 20%, 30%, 40% CO_2 concentrations

Reynolds Number versus momentum ratio scatter plots in figure 35 displayed clearly how changing CO_2 concentrations in biogas mixture affects the flame stability at each premixing ratio. It is obvious that at 0% CO_2 concentration in biogas mixture the Reynolds is highest at each premixing ratio scatter plot, while at 40% CO_2 concentration the Reynolds Number is minimum, and the scatter is almost following a vertical pattern. This happens because the presence of CO_2 dilutes the biogas mixture and absorbs heat from the reaction, thus decreasing the laminar burning velocity and Reynolds Number. In LD1, most of the scatter is shifted to the left because of the poor mixing in short premixing lengths which force the flow to acquire low momentum ratio at flame extinction. Regarding premixing ratios 3, 9, and 12, higher momentum ratios can be reached at 10% and 20% CO_2 concentrations in biogas mixture, otherwise the premixing length will not be enough to handle other higher CO_2 Concentrations as shown in figure 36. However, at premixing ratio 5, the highest momentum ratios indicating effective mixing were achieved by all CO_2 concentrations at corresponding high values of Reynolds Number. Premixing ratios 15 and 12 achieved almost the same range of momentum ratios and Reynolds Number. But in LD15 the 30% and 40% CO_2 Concentrations in biogas mixture, showed a bit higher momentum ratio level at same Reynolds Numbers range as shown in figure 36.

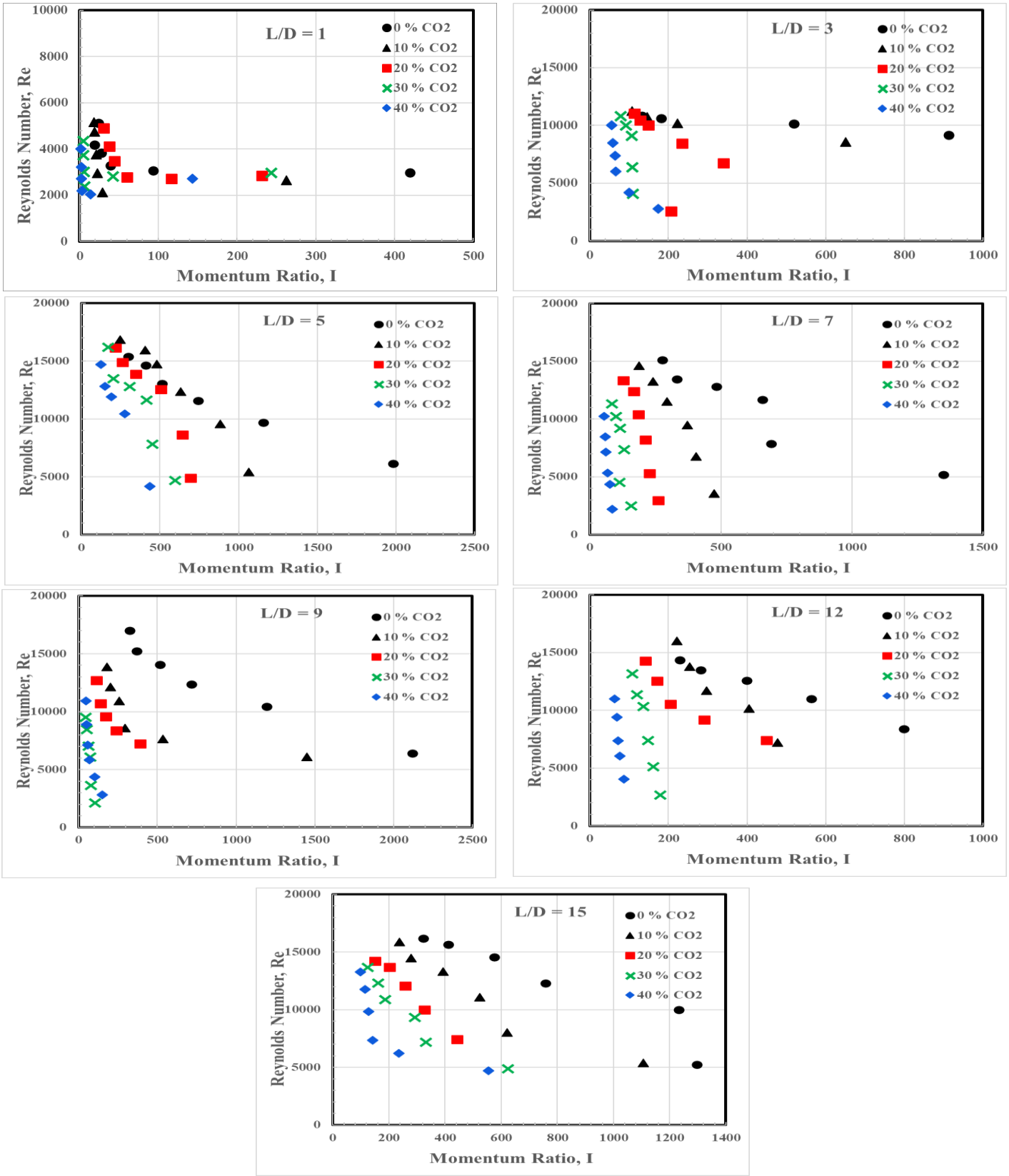

Figure 36: Plots of Reynolds number against momentum ratio at fixed premixing ratio values of 1, 3, 5, 7, 9, 12, 15

4.5 Biogas Flame Temperature Analysis

The temperature of the flame was studied for all CO_2 concentrations contained in biogas mixture at different vertical levels from the burner's nozzle. The flame temperature was measured at both premixing ratios 7 and 15 to address the difference. A stable flame operating parameter was set by choosing any point below the stability curves in figures 29 and 30. Flame was set at turbulent conditions with Reynolds Number of 4000 and equivalence ratio of 2. As mentioned earlier, a B type thermocouple was used and mounted above the middle of the 60 mm nozzle length and moved by steps of 0.5 mm along the x-axis mentioned in figure 25 and illustrated by figure 28. The temperature measurements were recorded at three vertical levels of 5mm, 30mm, and 60mm above the nozzle's exit as shown in table 7. Comparison between the three vertical levels for each CO_2 concentration and each premixing ratio was done as seen in figures 37 and 38. The measurements along the slot width were found to be symmetric about the slot's longitudinal axis of symmetry, so the origin (X = 0 mm) was taken at the center of the slot. The mirrored temperature variation about the axis of symmetry was removed and only one side was displayed. The temperature variation is different in the three vertical levels as seen in the figures, but the behavior of all variations at same vertical levels at different CO_2 concentrations and different premixing ratios looks the same. At 5 mm above the nozzle, the temperature has a bell shape profile on both sides of the center, indicating that there are two reaction zones. The two reaction zones found to be already merged at 30mm and 60mm above the burner's slot, as the temperature profile displays half a bell shape on one side of the center. The peak temperature increases as shown in all temperature variation graphs

when the thermocouple probe goes vertically upwards, indicating that enhanced mixing is achieved upwards.

Table 7: Way of recording temperatures at different positions and conditions

Premixing Ratio	CO_2%	Probe Positions along z-axis	Probe positions along x-axis					
			X=0mm	X=0.5mm	X=1mm	X=1.5mm	….. …… ……	X=30mm
LD=7	0%	0.5 mm						
		30 mm						
		60 mm						
	10%	0.5 mm						
		30 mm						
		60 mm						
	20%	0.5 mm						
		30 mm						
		60 mm						
	30%	0.5 mm						
		30 mm						
		60 mm						
	40%	0.5 mm						
		30 mm						
		60 mm						
LD=15	0%	0.5 mm						
		30 mm						
		60 mm						
	10%	0.5 mm						
		30 mm						
		60 mm						
	20%	0.5 mm						
		30 mm						
		60 mm						
	30%	0.5 mm						
		30 mm						
		60 mm						
	40%	0.5 mm						
		30 mm						
		60 mm						

Recorded Temperatures by Thermocouple

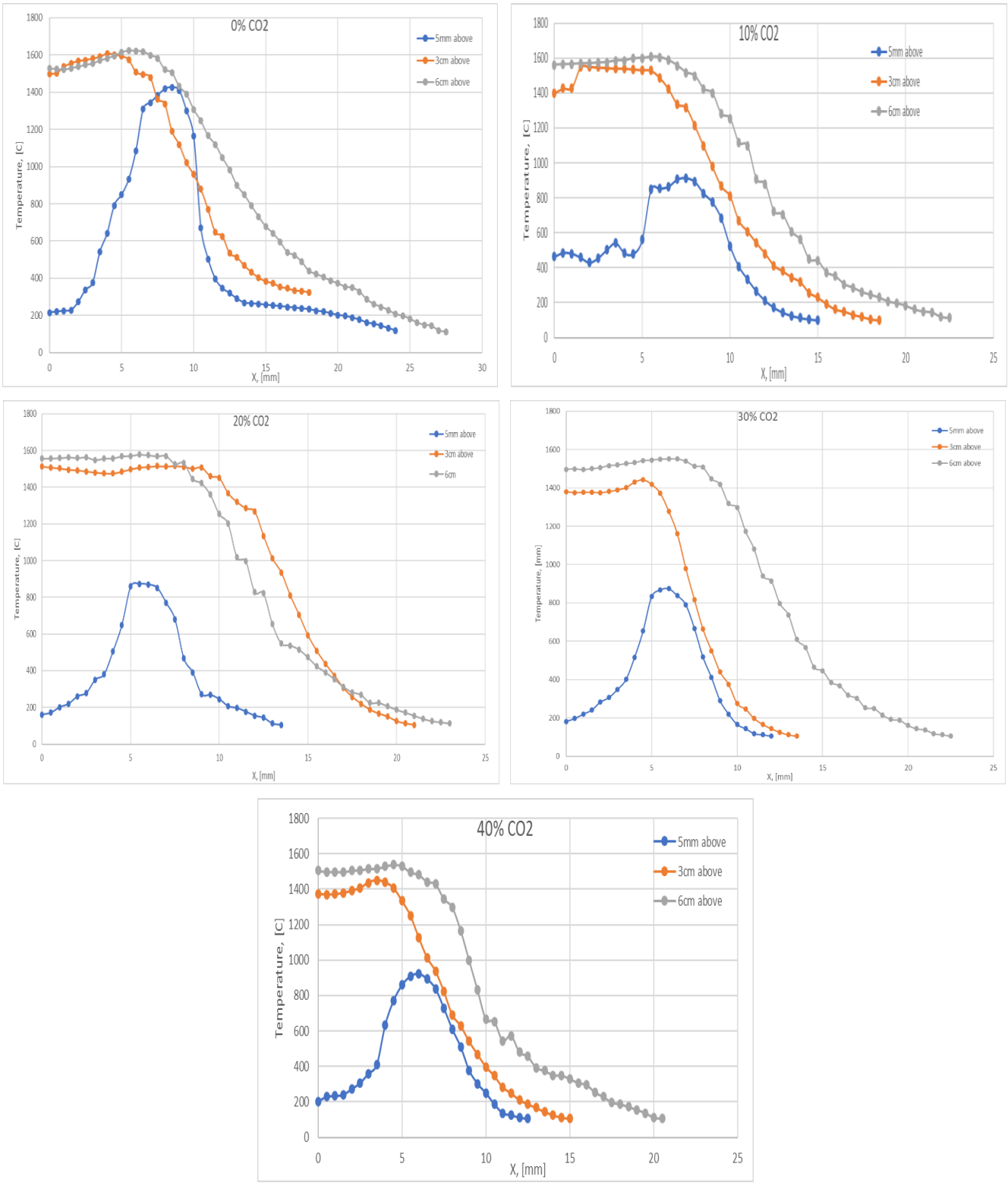

Figure 37: Temperature along x-axis at premixing ratio 7 for 0%, 10%, 20%, 30%, 40% CO_2 concentrations

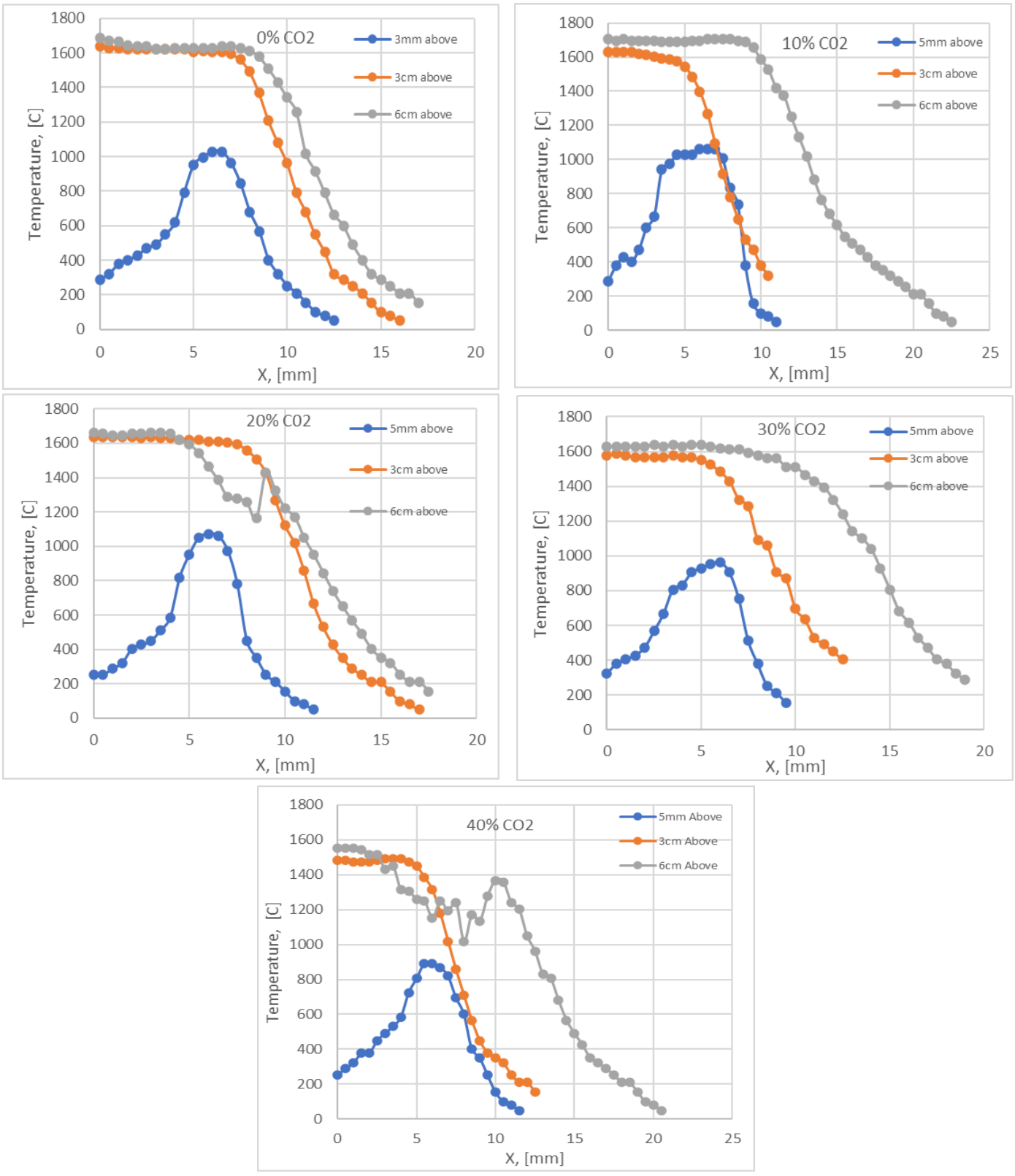

Figure 38: Temperature along x-axis direction at premixing ratio 15 for 0%, 10%, 20%, 30%, 40% CO_2 concentrations

Maximum temperature of all curves was recorded for each CO_2 Concentration, premixing ratio, and vertical height. To study the effect of increasing CO_2 proportion in biogas mixture on maximum flame temperature, the maximum temperature was plotted against CO_2 concentration at fixed premixing ratio and height above the nozzle. At all CO_2 concentrations and at a fixed height level equal 5mm, premixing ratio of 15 achieved higher temperature than LD7. However, at 30mm and 60mm height levels LD7 acquired higher temperatures at all CO_2 concentrations as shown in figure 39. As predicted, the highest temperature was achieved at 100% NG without CO_2 presence at both premixing ratios. At 5mm vertical level, the temperature at 0% CO_2 and LD15 was higher than 20%, 30% and 40% CO_2 concentrations by 88C, 204C, and 424C respectively. While at LD7, the temperature at 0% CO_2 was higher than 20%, 30% and 40% CO_2 concentrations by 21C, 74C, and 199C respectively. At 30mm above nozzle and LD7, the temperature at 0% CO_2 was higher than 30% and 40% CO_2 concentrations by 26C and 129C respectively. While at LD15, the temperature at 0% CO_2 was higher than 30% and 40% CO_2 concentrations by 88C and 84C respectively. The above-mentioned data agrees with Ghenai et al. [23], as the biogas obtained from digester at both CO_2-methane ratio 0.89 and 0.54 led to a flame temperature decrease by 37% and 22% respectively compared to flame temperature by natural gas. Abdel-hadi [29] obtained biogas from cattle dung and chicken manure which also resulted in a low peak flame temperature of 460C and 631C for methane content of 54.5% and 68.1% respectively.

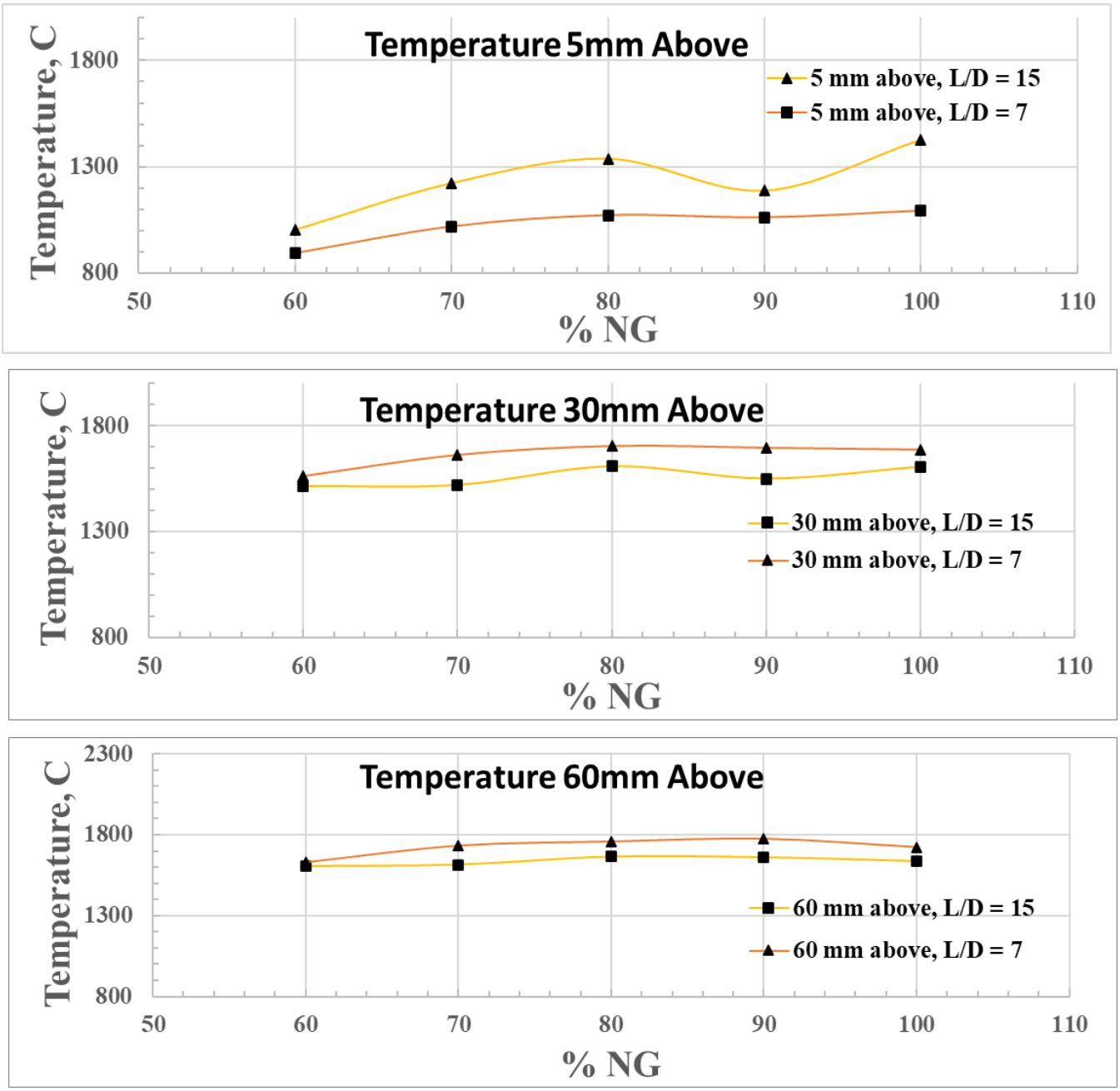

Figure 39: Peak temperature versus natural gas concentration at height levels of 5mm, 30mm, 60mm above burner's nozzle

As the 3D mechanism goes up with the thermocouple, the reading in mV was found to increase as shown in figure 40. The temperature increases with a larger increment when moving from 5 mm to 30 mm above the nozzle level in comparison to moving from 30 mm to 60 mm. The reason behind this is the presence of two reaction zones at 5 mm above that were merged at 30 mm height level, thus giving a much higher temperature value. It is clearly noticed from the figures below that the temperature increases in all cases when the thermocouple goes up through the flame. Besides, as the CO_2 concentration in biogas mixture increases the curve shifts down in both premixing ratios of 7 and 15.

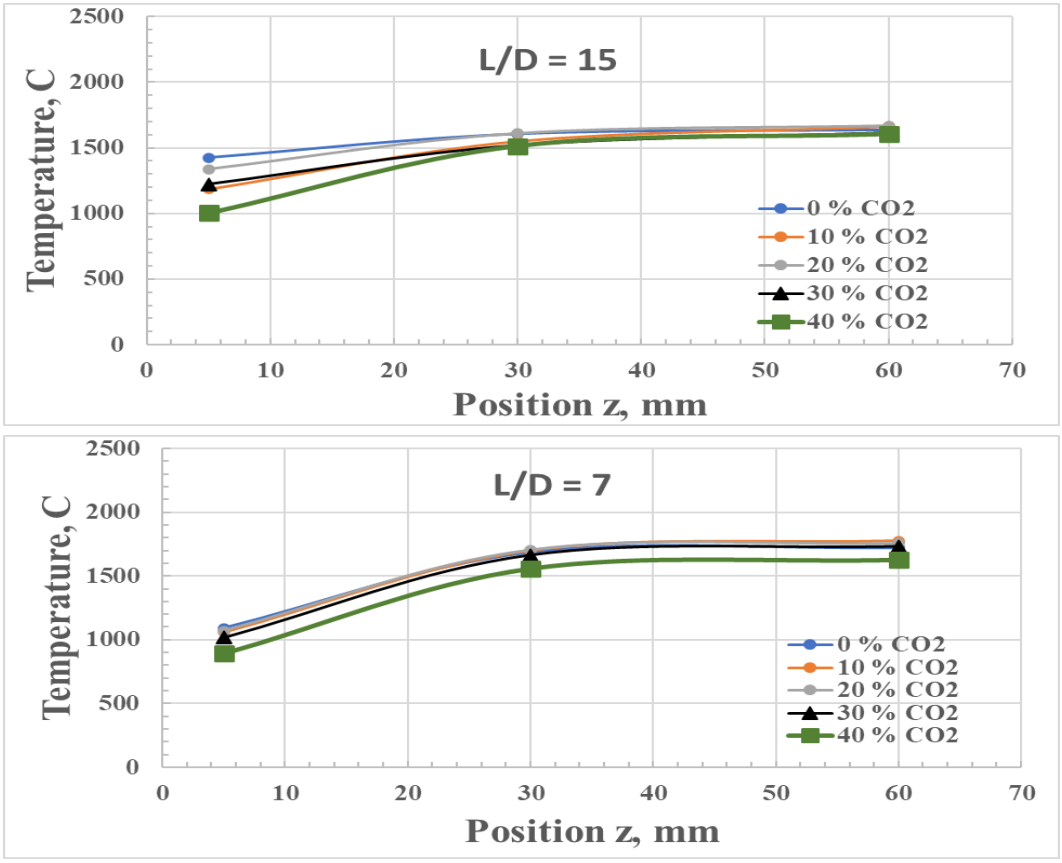

Figure 40: Temperature variation along z axis for premixing ratios LD7 and LD15

Flames at premixing ratio of 15 were captured from the front and the side view at all CO_2 concentrations contained in biogas mixtures. All flames were adjusted at same Reynolds number of 4000 and equivalence ratio of 2. The flame decreases in height from left to right when the CO_2 concentration is increased, as shown from the flame front view images in figure 41. Also, the flame's blue color fades and becomes lighter once the CO_2 concentration is increased in the biogas mixture, and this is clear from the flame side view shots. This observation supports the results obtained by Ilminnafik et al. [30], as flame of biogas used before purification (more CO_2 content) achieved lighter blue color in comparison with the flame obtained from purified biogas which has lower CO_2 content. The cause behind this behavior is that the presence of CO_2 lead to frequent collisions with fuel molecules which in turn decreases the number of ions formed and so the color of the flame becomes lighter [30].

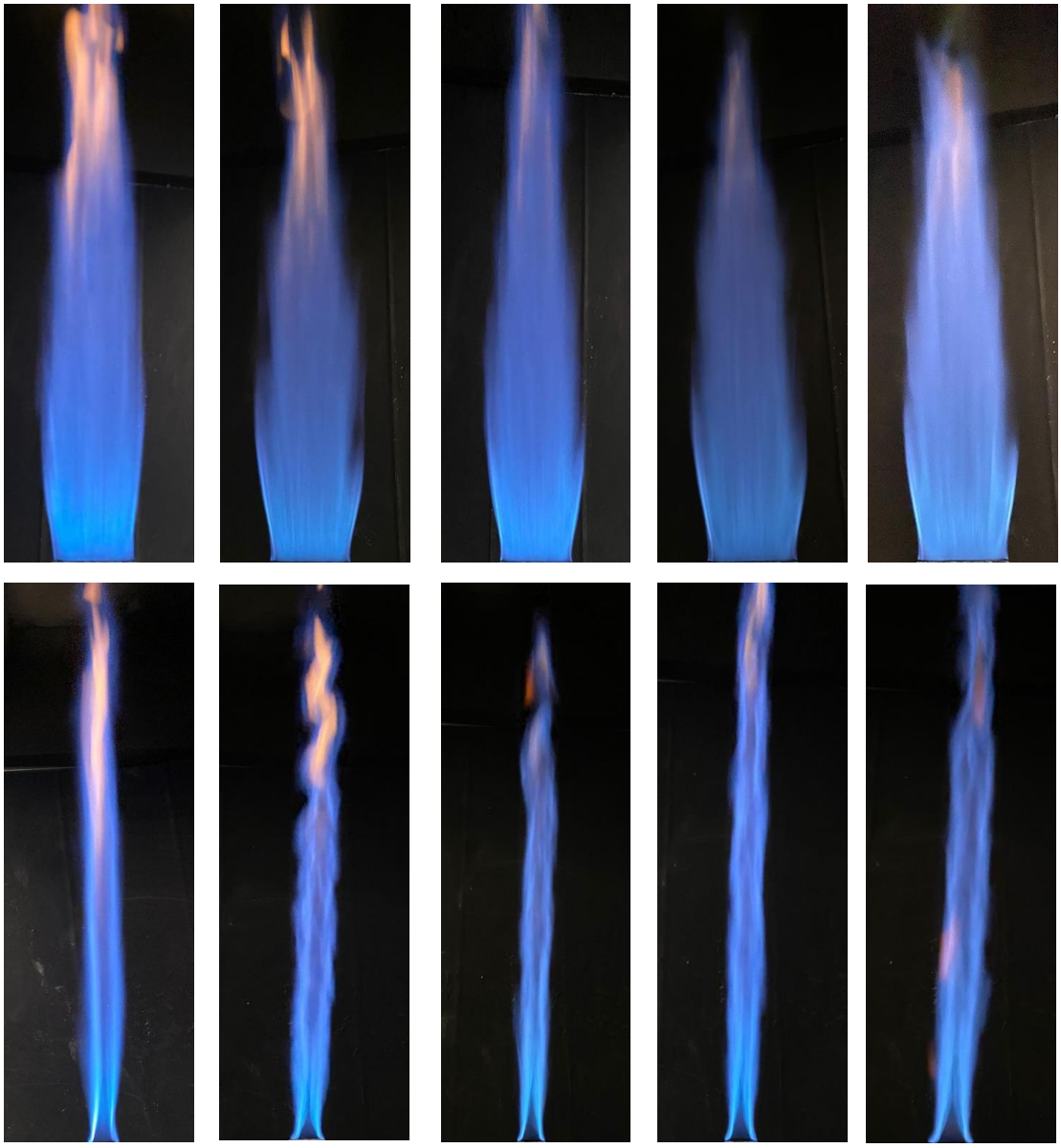

Figure 41: Front and side view flame images at 0%, 10%, 20%, 30%, 40% CO_2 concentrations from left to right respectively

Conclusion

Highest flame stability obtained by biogas mixture is achieved at a specific level of mixture inhomogeneity between non premixed and fully premixed conditions. Premixing ratio of 5 didn't show best flame stability during the absence of CO_2 in comparison with other premixing ratios, but when CO_2 concentration is increased from 10% to 40% premixing ratio of 5 achieved highest Reynolds number. Meaning that partial premixing was effective on biogas mixture due to the creation of rich and lean pockets throughout the flow, which prevents local flame extinctions at high turbulent conditions.

As predicted, flame stability decreases as the CO_2 concentration in biogas increases. Meaning that the flame reaches low values of Reynolds number and equivalence ratio at the blowout. This happened due to the low heating value of biogas and the temperature diluting effect of CO_2.

Besides, the flame stability was found to decrease as the velocity and momentum ratio of the flow increases. The Reynolds number is almost decreasing linearly by increasing the momentum ratio under all CO_2 concentrations and LDs.

Finally, the temperature was found to decrease when CO_2 concentration is increased. The centerline temperature of flames at all CO_2 concentrations was found to increase steeply as the thermocouple probe moves vertically upward from 5 mm to 30 mm above the nozzle, while it didn't increase as much when the probe was moved from 30 mm to 60 mm upwards. This behavior is due to the merging of two reaction zones at higher vertical levels between 5 mm and 30 mm above the nozzle, thus yielding a steep increase in temperature.

Future Works

More investigations regarding biogas combustion will still need to be done. All flames were investigated at constant air co-flow speed of 5 m/s, so higher co-flow speeds need to be investigated to look for more stable flames. Secondly, the temperature of flame needs to be measured in smaller steps along the vertical direction above the nozzle, as the temperature was only measured at three vertical levels of 5 mm, 30 mm, and 60 mm to study the temperature variation more. Thirdly, temperature was also measured for LD7 and LD15 only, so the temperature needs to be addressed for other hollow chambers of LD3, LD5, LD9, and LD12. Finally, the whole analysis done on the current burner needs to be also done on another burner with different air and fuel nozzle widths, like widths of 2 mm, 4 mm, 2 mm instead of 1 mm, 6 mm, 1 mm section widths.

References

[1] Bond Tom, Templeton Michael R. History and Future of Domestic Biogas Plants in the Developing World. Energy for Sustainable Development 2011;15:347-354.

[2] Kriaučiūnas Donatas, Pukalskas Saugirdas, Rimkus Alfredas, Barta Dalibor. Analysis of the Influence of CO_2 Concentration on a Spark Ignition Engine Fueled with Biogas. Applied Sciences 2021;11:1-16.

[3] El-Mahalawy Fawzy, Abdelhafez Ahmed, Mansour Mohy S. Mixing and Nozzle Geometry Effects on Flame Structure and Stability. Combustion Science and Technology 2007;179:249-263.

[4] Mansour Mohy S. Stability Characteristics of Lifted Turbulent Partially Premixed Jet Flames. Combustion and Flame 2003;133:263-274.

[5] Mansour Mohy S. The Flow Field Structure at the Base of Lifted Turbulent Partially Premixed Jet Flames. Experimental Thermal and Fluid Science 2004;28:771-779.

[6] Elbaz A.M., Zayed M.F., Samy M., Roberts W.L., Mansour M.S. Te Flow Field Structure of Highly Stabilized Partially Premixed Flames in a Concentric Flow Conical Nozzle Burner with Coflow. Experimental Thermal and Fluid Science 2016;73:2-9.

[7] Abdallah Muhammed S., Mansour Mohy S., Allam Nageh K. Mapping the Stability of Free-Jet Biogas Flames Under Partially Premixed Combustion. Energy 2021;220:119749.

[8] Suprianto Fandi Dwiputra, Anggono W., Tanoto M.S.C. Effect of Carbon Dioxide on Flame Characteristics in Biogas External Premix Combustion. International Journal of applied Engineering Research 2016;11:2240-2243.

[9] Cacua Karen, Amell Andres, Cadavid Francisco. Effects of Oxygen Enriched Air on the operation and Performance of a Diesel-Biogas Dual Fuel Engine. Biomass and Bioenergy 2012;45:159-167.

[10] Anggono Willyanto, Suprianto Fandi Dwiputra, Wijaya Tubagus, Tanoto Michael S.C. Behavior of Flame Propagation in Biogas Spark Ignited Premix Combustion with Carbon Dioxide Inhibitor. Advanced Materials Research 2014;1044-1045:251-254.

[11] Anggono Willyanto, Wardana I.N.G., Lawes M., Hughes Kevin. Effect of Inhibitors on Biogas Laminar Burning Velocity and Flammability Limits in Spark Ignited Premix Combustion. International Journal of Engineering and Technology 2013;5:4980-4987.

[12] Kobayashi Hideaki, Hagiwara Hirokazu, Kaneko Hideaki, Ogami Yasuhiro. Effects of CO_2 Dilution on Turbulent Premixed Flames at High Pressure and High Temperature. Proceedings of the Combustion Institute 2007;31:1451-1458.

[13] Anggono Willyanto, Wardana I. N. G., Lawes M., Hughes K. J., Wahyudi Slamet, Hamidi Nurkholis, Hayakawa Akihiro. Biogas Laminar Burning Velocity and Flammability Characteristics in spark Ignited Premix Combustion, Journal of Physics: Conference Series 2013;423:012015.

[14] Anggono Willyanto, Wardana I. N. G., Lawes M., Hughes K. J., Wahyudi Slamet, Hamidi Nurkholis. Laminar Burning Velocity and Flammability Characteristics of Biogas in Spark Ignited Premix Combustion at Reduced Pressure. Applied Mechanics and Materials 2013;376:79-85.

[15] Anggono Willyanto, Wardana I. N. G., Lawes M., Hughes K. J., Wahyudi Slamet, Hamidi Nurkholis. Laminar Burning characteristics of Biogas-Air Mixtures in Spark Ignited Premix Combustion. Journal of Applied Sciences Research 2012;8:4126-4132.

[16] D'Auzay, Charles Turquand, Papapostolou V., Chakraborty Nilanjan. Effects of Biogas Composition on the Edge Flame Propagation in Igniting Turbulent Mixing Layers. Flow Turbulence and Combustion 2021;106:1437-1459.

[17] Elbaz Ayman M., Mansour Mohy M., Akoush Bassem M, Juddoo Mrinal, Khedr Alaa M., AlBulqini Hazem M., Zayed Mohamed F., Ahmed Mahmoud M.A., Roberts William L., Masri Asaad R. Detailed Investigation of the Mixing Field and Stability of Natural Gas and Propane in Highly Turbulent Planar Flames. Fuel 2022;309:122222.

[18] Mansour Mohy M., Elbaz Ayman M., Roberts William L., Zayed Mohamed F., Juddoo Mrinal, Akoush Bassem M, Khedr Alaa M., AlBulqini Hazem M., Masri Asaad R. Structure and Stability Characteristics of Turbulent Planar Flames with Inhomogeneous Jet in a Concentric Flow Slot Burner. Proceedings of the Combustion Institute 2021;38:2597-2606.

[19] Raboni Massimo, Viotti Paolo, Capodagilo Andrea G. A comprehensive analysis of the current and future role of biofuels for transport in the European Union (EU). Ambiente & Agua – An Interdisciplinary Journal of Applied Science 2014;10.

[20] Baudoin E., Bai X. S., Yan B., Liu C., Yu R., Lantz A., Hosseini S. M., Li B., Elbaz A., Sami M., Li Z. S., Collin R., Chen G., Fuchs L., Alden M., Mansour M. S. Effect of Partial Premixing on Stabilization and Local Extinction of Turbulent Methane/Air Flames. Flow Turbulence and Combustion 2013;90:269-284.

[21] Rashwan Sherif S., Essawey Abdelmaged H. Ibrahim, Abou-Arab Tharwat W Abou, Nemitallah Medhat, Habib M. A. Experimental investigation of partially premixed methane-air and methane-oxygen flames stabilized over a perforated-plate burner. Applied Energy 2016;169:126-137.

[22] Liu Yu, Xue Qingguo, Zuo Haibin, Yang Fan, Peng Xing, Wang Jingsong. Effects of CO2 and N2 Dilution on the Combustion Characteristics of H2/CO Mixture in a Turbulent, Partially Premixed Burner. ACS Omega 2021;6:24:15651-15662.

[23] Ghenai Chaouki, Janajreh Isam. Combustion of Renewable Biogas Fuels. Journal of Energy and Power Engineering 2015;9:831-843.

[24] Cueller Amanda D., Webber Michael E., Cow Power: The Energy and Emissions Benefits of Converting Manure to Biogas. Environment Research Letters 2008;10.1088:1748-9326.

[25] Simsek Suleyman, Uslu Samet, Simsek Hatice. Experimental study on the ability of different biogas level dual fuel spark ignition engine: Emission mitigation, performance, and combustion analysis. Oil & Gas Science and Technology 2021;76:74.

[26] Kim Yungjin, Kawahara Nobuyuki, Tsuboi Kazuya, Tomita Eiji. Combustion characteristics and NOX emissions of biogas fuels with various CO2 contents in a micro co-generation spark-ignition engine. Applied Energy 2016;182:539-547.

[27] Wang Kuanliang, Li Fei, Zou Pengfei, Lin Xin, Ronghai Mao, Yu Xilong. Effect of the fuel-air flow velocity on heat release rate of swirling non-premixed methane flames. Aerospace Science and Technology 2019;95:105465.

[28] Mastrodonato Arianna, Borm Oliver. Impact of the Air to Fuel Jet Momentum Ratio on the NOx Emissions of a Hydrogen Combustion Chamber. Conference: European Combustion Meeting 2015.

[29] Abdel-Hadi M.A. Determination of Methane Content by Measurements of Flame Temperature and Voltage from Biogas Burner. Misr Journal of Agriculture Engineering 2009;26:498-513.

[30] Ilminnafik Nasrul, Setiyawan D. L., Sutjahjono H., Rofiq A., Hadi A. S. Flame Characteristics of Biogas From Coffee Waste Materials. Journal of Physics Conference Series 2019;10.1088:1742-6596.